(NASA-CR-142553) [RESEARCH ON FLUORESCENCE FROM PHOTOIONIZATION, PHOTODISSOCIATION, AND VACUUM, ALONG WITH BENDING QUANTRUM STUDY] Progress Reports, 1 Nov. 1971 - 31 Oct. 1974 (University of Southern Calif.) 108 p HC G3/72 18041

N75-21091

Unclas

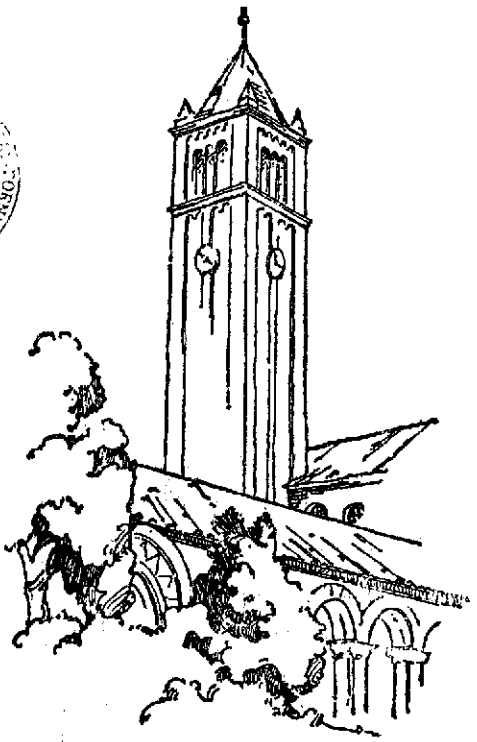

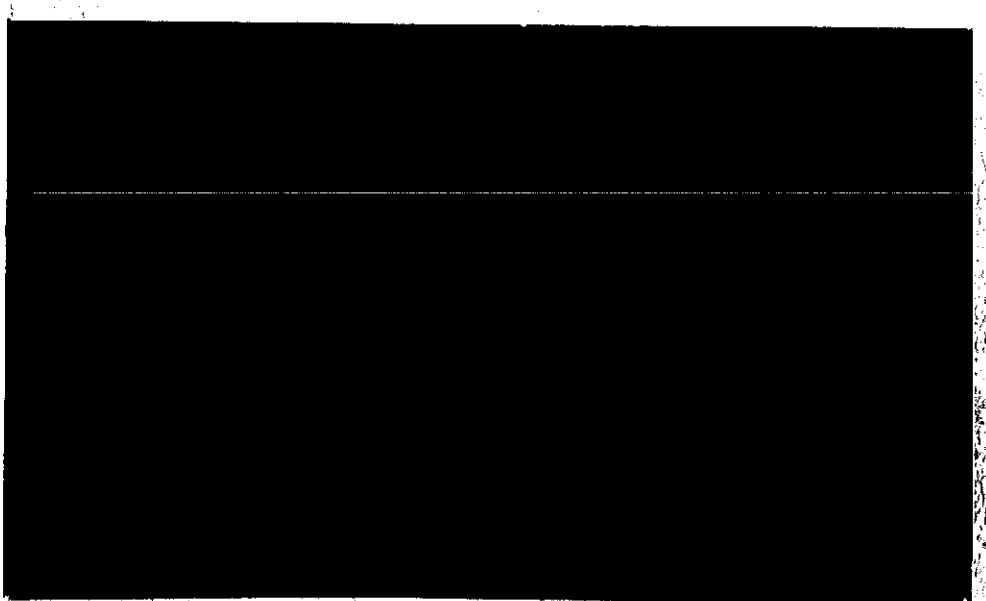

DEPARTMENT OF PHYSICS
University of Southern California
Los Angeles, California 90007

Progress Report No.:	Period Covered:
4 and 5	11/1/71-10/31/72
6 and 7	11/1/72-10/31/73
8 and 9	11/1/73-10/31/74

PROGRESS REPORTS NO. 4, 5, 6, 7, 8 AND 9 FOR THE PERIOD ENDING OCTOBER 31, 1974

Grant # NGR 05-018-180

Darrell L. Judge
Principal Investigator
University of Southern California
Los Angeles, California 90007

1 April 1975

TABLE OF CONTENTS

* Reprints intentionally Omitted

XIII. "$CS(A^1\Pi \rightarrow X^1\Sigma^+)$ Fluorescence from Photodissociation of CS_2 and OCS," submitted to J. Chem. Phys. 1974.

XIV. "$OCS^+(A^2\Pi \rightarrow X^2\Pi)$ Fluorescence from Photoionization of OCS," accepted for publication in Int. J. Mass Spectrometry Ion Phys. 1975.

XV. "Reevaluation of the $CO_2^+(X^2\Pi_g)$ Bending Quantum," accepted for publication in Can. J. Phys. 1975.

APPENDIX A

Continuation Proposal, April 26, 1972.

APPENDIX B

Continuation Proposal, July 10, 1973

SECOND INTERNATIONAL

CONFERENCE

ON

SPECTRAL LINES

Sponsored by the
Division of Electron and Atomic Physics
of the American Physical Society

M.7 Fluorescence from the Fragment of CS_2 Vapor Produced by Vacuum Ultraviolet Radiation, L.C. LEE and D.L. JUDGE, Univ. of So. Calif.--The fluorescence from the photo-fragments of CS_2 produced by line emission sources at wavelengths between 462 and 1239 Å has been studied. The fluorescence emitted from the transitions of $CS_2^+(B^2\Sigma_u^+ \rightarrow X^2\Pi_g)$, $CS_2^+(A^2\Pi_u \rightarrow X^2\Pi_g)$ and $CS(A^1\Pi \rightarrow X^1\Sigma)$ has been observed and the corresponding emission band strengths and production cross sections measured. From the $CS(A^1\Pi \rightarrow X^1\Sigma)$ emission spectrum the populations of vibrational levels of CS photo-fragments in the $A^1\Pi$ electronic state have been obtained. The vibrational population of the $v' = 0$-4 levels are well represented by a Poisson distribution, in agreement with a theoretical argument.

$CS_2^+(B^2\Sigma_u^+, A^2\Pi_u \rightarrow X^2\Pi_g)$ FLUORESCENCE FROM PHOTOIONIZATION EXCITATION OF CS_2 VAPOR

L. C. Lee, D. L. Judge and M. Ogawa

Department of Physics
University of Southern California
Los Angeles, California 90007

Index classification: 5.447

Abstract

$CS_2^+(B^2\Sigma_u^+, A^2\Pi_u \rightarrow X^2\Pi_g)$ fluorescence bands produced by irradiation of CS_2 vapor with emission lines from $\lambda\lambda$462-977 Å were analyzed and their production cross sections measured. The emission bands of the bending transitions, $B^2\Sigma_u^+(0v0) \rightarrow X^2\Pi_g(0v0)$, were tentatively assigned and ν_2 of the $B^2\Sigma_u^+$ state is accordingly found to be 338.8 cm^{-1}. Using the tentatively assigned positions of the band heads for the $A^2\Pi_u(v00) \rightarrow X^2\Pi_g(000)$ transitons the ionization potentials for the $A^2\Pi_u(v00)$ vibrational levels were obtained and are in a good agreement with the photoelectron data. The splitting constant of the spin-orbit interaction for the $A^2\Pi_u$ state thereby determined to be 169 cm^{-1}. The $CS_2^+(A^2\Pi_u^+, B^2\Sigma_u \rightarrow X^2\Pi_g)$ fluorescence has exceptionally high production cross sections at the absorption bands associated with the n=3 member of the Rydberg series III and V, respectively.

I. Introduction

Fluorescence emission from CS_2^+ was observed by Cook and Ogawa (1969) following irradiation of the CS_2 molecule by photons of the wavelengths shorter than λ976.5 Å. Such fluorescence produced by λ955 Å photons has been dispersed and reported by Weissler et al. (1971), the fluorescence being identified as the CS_2^+ ($A^2\Pi_u \rightarrow X^2\Pi_g$) system. However, due to the spectral resolution limitation the most interesting features of the spectrum were not revealed.

Using various techniques the ionization potentials of the CS_2^+ ions in the $B^2\Sigma^+_u$, $A^2\Pi_u(i)$, and $X^2\Pi_g(i)$ electronic states have been studied by several authors: Price and Simpson (1932), Tanaka et al. (1960), and Ogawa and Chang (1970) have investigated the Rydberg series and obtained the ionization potentials from the series limits; Callomon (1958) studied the emission spectrum of the $CS_2^+(B^2\Sigma^+_u \rightarrow X^2\Pi_g)$ system; Diebeler and Walker (1967) and Momigny and Delwiche (1968) have investigated the mass spectra of the CS_2^+ ions ionized by photoabsorption; Turner and May (1967), Eland and Dunby (1968), Collin and Natalis (1968), and Brundle and Turner (1969) have studied the photoelectron spectra resulting from the photoionization of CS_2 by the λ584 Å helium resonance line. Through such observations the nature of the CS_2^+ electronic states is reasonably well understood. However, due to the lack of high resolution rotational analysis of the $B^2\Sigma^+_u \rightarrow X^2\Pi_g$ and

$A^2\Pi_u \rightarrow X^2\Pi_g$ emission systems, the precise positions of the vibrational levels of those states are still not established, and further study of these systems is required.

Carbon disulfide is one of the molecules of astrophysical and aeronomic interest (Hudson, 1970). Measurement of the production cross sections for the $CS_2^+(B^2\Sigma_u^+, A^2\Pi_u \rightarrow X^2\Pi_g)$ fluorescence, produced by vacuum ultraviolet radiation is thus of considerable interest. Such data will provide basic information for an understanding of the role CS_2 plays in planetary atmospheres.

II. Experiment

The experimental set-up has been described in a previous paper (Judge and Lee, 1972). In brief, the light source is a condensed spark discharge through a boron nitride capillary containing either N_2 or Ar. The emission lines of interest were isolated with a 1-m normal incidence monochromator (McPh. 225). The fluorescence was dispersed by a 0.3-m monochromator (McPh. 218), with the bandwidth set at 5 Å or less.

The source line intensities were measured with a nickel film detector for which the quantum efficiency was known (Walker et al., 1955). For the absolute intensity measurement of fluorescence the response of the combination of a grating blazed at 5000 Å and a cooled photomultiplier (EMI 9558 QB) in the wavelength region λλ3000-7000 Å was calibrated with an EG&G tungsten halogen lamp.

The response curve is similar to that published in a previous paper (Lee and Judge, 1972). The second order spectrum of the $B^2\Sigma_u^+ \rightarrow X^2\Pi_g$ emission in the region $\lambda\lambda$2750-2950 Å was observed. The response in this region was calibrated against sodium salicylate, for which the quantum efficiency is known (Slavin et al., 1961). The system response was found to be reasonably constant.

CS_2 vapor was obtained from an analytical-reagent-grade liquid CS_2. The vapor was purified by fractional distillation so that the fluorescence from the possible impurities, especially N_2, produced by irradiation of λ555 Å was not detectable. The vapor pressure inside the sample cell was monitored with a Baratron Capacitance manometer and was limited to 15 mTorr or less so that the fluorescence intensity was linearly proportional to the pressure.

III. Result and Discussion

A. $B^2\Sigma_u^+ \rightarrow X^2\Pi_g$ System

The $B^2\Sigma_u^+ \rightarrow X^2\Pi_g$ fluorescence spectra produced by irradiation of photons with wavelengths λ555, 827, 835, and 851 Å are shown in Figure 1. The spectrum produced by λ555 Å radiation is characteristic of all observed spectra produced by photons with wavelengths not longer than λ827 Å. The observed positions of band heads, the wave numbers, and the relative production cross sections for the various emission bands are listed in Table I.

The bands a to y shown in Figure 2 have been observed by

Callomon (1958) who obtained the emission spectrum from the negative flow of a d.c. discharge through CS_2 vapor. The rotational spectrum of the a and b bands has been analyzed by Callomon (1958) and assigned respectively to the $B^2\Sigma_u^+(000) \rightarrow X^2\Pi_{g,3/2}(000)$ and $X^2\Sigma_{g,1/2}(000)$ transitions. The p band has a rotational spectrum similar to the a band and is thus assigned to the $B^2\Sigma_u^+(000) \rightarrow X^2\Pi_{g,3/2}(020)$ transition. Callomon (1958) also suggested that the e and f bands correspond to the $B^2\Sigma_u^+(000) \rightarrow X^2\Pi_{g,3/2}(100)$ and $X^2\Pi_{g,1/2}(100)$ transitions. The correctness of this suggestion is corroborated by the presently observed spectra. Because the a, b, e, and f bands are emitted from the same upper level, $B^2\Pi_u^+(000)$, their relative emission cross sections will be independent of the incident photon energy. This independence is apparently consistent with the present spectra shown in Figure 1 and listed in Table I.

As shown in Figure 2, the spearations of the α-β and the c-d bands are the same as that of the a-b bands. And, the intensity distribution of the α, c, and a bands is similar to that of the β, d, and b bands. Considering the uniformity of the band separations these bands may thus be vibrational progressions. As shown in Figure 1 the α, c, β, and d bands are not produced by primary photons having wavelengths shorter than λ835 Å; their production is strongly dependent on the primary photon energies. This may imply that these bands are emitted from the various vibrational levels of the upper $B^2\Sigma_u^+$ state, of which the formation is dependent

on the primary photon energy.

The bending vibration transition, $B^2\Sigma_u^+(010) \rightarrow X^2\Pi_g(010)$ has been observed in the BO_2 molecule by Johns (1961). Since the CS_2^+ ion is isoelectronic (Callomon, 1958, Johns, 1961) to the BO_2 molecule, the $CS_2^+[B^2\Sigma_u^+(0v'0) \rightarrow X^2\Pi_g(0v''0)]$ transitions are thus to be expected. In fact, in considering the combination of the vibrational frequencies for the $B^2\Sigma_u^+ \rightarrow X^2\Pi_g$ transitions, only the $(0v'0) \rightarrow (0v''0)$ transitions can possibly explain the separations of the c-a and d-b bands which are given by Callomon (1958) as 134.04 and 137.27 cm^{-1}, respectively. The ν_1 vibrational frequency of the $B^2\Sigma_u^+$ has been determined by photoelectron spectroscopy (Eland and Danby, 1968, Brundle and Turner, 1969) to be 605 cm^{-1}, which is comparable to ν_1(= 623.94 cm^{-1}) of the $X^2\Pi_g$ state given by Callomon (1958). The ν_3 vibrational frequencies are still unknown for both the $B^2\Sigma_u^+$ and $X^2\Pi_g$ state. However, according to the data ν_1 = 1070 cm^{-1} and ν_3 = 1322 cm^{-1} for the $BO_2(X^2\Pi_g)$ state, ν_3 for the $CS_2^+(X^2\Pi_g)$ state is expected to be of the order of ν_1. From these considerations the possibility that the α, c, β, and d bands are emitted from the most likely populated levels, $B^2\Sigma_u^+(v00)$, is ruled out. The Frank-Condon factors for the productions of the $CS_2^+(B^2\Sigma_u^+)$ ions in the (000), (100), and (200) levels have been determined by λ584 Å photoelectron spectroscopy (Brundle and Turner, 1969) to be 0.89, 0.10, and 0.01, respectively.

According to the vibrational selection rules for electronic

transition (Herzberg, 1966) $\Delta V_2 = 0, \pm 2, \pm 4, ---$, the bending vibrational levels of the $CS_2^+(B^2\Sigma_u^+)$ electronic state can only be populated by excitation of the neutral molecules in the bending vibrational levels of the ground electronic state. Since the $\Delta V_2 = 0$ are usually the strongest transitions (Herzberg, 1966), the populations in the bending vibrational levels of the upper electronic state will approximately have the same distribution as that of the ground electronic state, whenever the electronic transition moment is assumed constant. In fact, as indicated in Table I, the relative production cross sections for the a: c: α or b: d: β bands (= 1.0: 0.16: 0.03), which are in turn proportional to the populations of the vibrational elevels, do indeed agree with the population distribution of the bending vibrational levels in the ground electronic state. THe bending vibrational frequency ν_2 for the $CS_2(X^1\Sigma_g^+)$ ground state (Herzberg, 1966) is 396.7 cm^{-1}, which results in a calculated Boltzman population distribution for the vibrational levels, (000): (010): (020) of 1: 0.14: 0.02, respectively. This fact also suggests that the c and α or the d and β bands may be emitted, respectively, from the bending vibrational levels, (010) and (020) of the $B^2\Sigma_u^+$ state. And the corresponding lower levels for these bands will be the (010) and (020) levels of the $X^2\Pi_g$ state whichare again determined by the selection rules, $\Delta V_2 = 0, \pm 2$, ---. The result for the suggested assignment is listed in Table I and also indicated in Figure 2. From this tentative assignment

and the ν_2 bending vibrational frequency (Callomon, 1958) (=204.8 cm^{-1}) of the $X^2\Pi_{g,3/2}$ state, ν_2 of the $B^2\Sigma_u^+$ state is thus 338.8 cm^{-1}. Similarly, ν_2 for the $B^2\Sigma_u^+$ state is larger than that for the $X^2\Pi_g$ state in the BO_2 molecule (Johns 1961), for which ν_2 values are, respectively, 505 and 464 cm^{-1}.

Production of the α, c, β, and d bands is strongly dependent on the incident wavelengths near λ835 Å. These wavelengths are in a region (λλ820-840 Å) where a strong and rather broad absorption feature is observed (Cook and Ogawa, 1969). This coincidence suggests that the $CS_2^+(B^2\Sigma_u^+)$ ions in the bending vibrational levels may not be produced by direct photoionization.

B. $A^2\Pi_u \rightarrow X^2\Pi_g$ System

The fluorescence spectrum in the wavelength region λλ4300-5800 Å produced by irradiating CS_2 vapor with photons of wavelength λ923 Å is shown in Figure 3. This spectrum is characteristic of all the observed spectra produced by photons of wavelengths not longer than λ955 Å.

The present spectrum has been identified as the $CS_2^+(A^2\Pi_u \rightarrow X^2\Pi_g)$ system (Weissler, 1971). However, this emission system is relatively unknown, in contrast to the isoelectronic systems, $CO_2^+(A^2\Pi_u \rightarrow X^2\Pi_g)$ and $BO_2(A^2\Pi_u \rightarrow X^2\Pi_g)$, which have been rotationally analyzed by Mrozowski (1941, 1942, 1947a,b) and Johns (1961), respectively. From the analysis of the $CS_2^+(B^2\Sigma_u^+ \rightarrow X^2\Pi_g)$ system Callomon (1958)

has determined that the vibrational levels of $X^2\Pi_{g,1/2}(000)$ and $X^2\Pi_{g,3/2}(000)$ are inverted, with a splitting of 440.71 cm^{-1}. On the other hand, the splitting in the vibrational levels of the $CS_2^+(A^2\Pi_u)$ state is not yet known. Although the ionization potentials for each vibrational level are well determined by photoelectron spectroscopy (Eland and Danby, 1968, Brundle and Turner, 1969), the splitting is not resolved.

In the $CO_2^+(A^2\Pi_u \rightarrow X^2\Pi_g)$ fluorescence spectra (Lee and Judge, 1972, Judge et al., 1969), the strong emission bands are grouped into sequences, $A^2\Pi_u(v00) \rightarrow X^2\Pi_g(v + m00)$, where $v + m \geq 0$, $v = 0$, 1, 2, --- and m is a fixed integer for each sequence. The band at the shorter wavelength side of each sequence is an $A^2\Pi_u(v00) \rightarrow X^2\Pi_g(000)$ transition. In analogy with the isoelectronic CO_2^+, the wavelengths for the $CS_2^+[A^2\Pi_u(v00) \rightarrow X^2\Pi_g(000)]$ transitions have been determined from the band head positions at the shorter wavelength side of each sequence and are listed in Table II. Combining the emission photon energies of these transitions with the ionization potentials of the $X^2\Pi_{g,1/2}(000)$ and $X^2\Pi_{g,3/2}(000)$ levels, which are respectively 81735 and 81299 cm^{-1} according to Tanaka et al. (1960), the ionization potentials for the vibrational levels of $A^2\Pi_u(v00)$ are obtained and listed in Table II. The ionization potentials given by other authors (Eland and Danby, 1968, Brundle and Turner, 1969, Ogawa and Chang, 1970) are also listed in the Table for comparison. The average value for the $\Omega = 1/2$ and $3/2$

components of each vibrational level agrees very well with the value given by Eland and Danby (1968). The splitting averaged over all vibrational levels is 0.021 eV (169 cm^{-1}). The uncertainty of the band head position is estimated to be ±5 Å resulting in an energy level uncertainty of 0.0025 eV.

It is interesting to compare the splittings of the Ω = 1/2 and 3/2 components of the isoelectronic molecules, CS_2^+, CO_2^+, and BO_2. The splittings for the $A^2\Pi_u(i)$ and $X^2\Pi_g(i)$ states are respectively 169 and 441 cm^{-1} (Callomon, 1958) for CS_2^+, 95 (Mrozowski, 1941, 1942, Tanaka and Ogawa, 1962) and 160 cm^{-1} (Bueso-Sanllehf, 1941) for CO_2^+, and 101 and 149 cm^{-1} for BO_2 (Johns, 1961).

Adopting the ν_1 values of the $CS_2^+(X^2\Pi_{g,1/2}$ and $X^2\Pi_{g,3/2})$ states from Callomon (1958), which are given, respectively, 631.06 and 616.82 cm^{-1}, and the ionization potentials of the $X^2\Pi_g$ states from Tanaka et al. (1960), the ionization potentials for the $X^2\Pi_g(v00)$ states may be obtained. Combining these ionization potentials with the presently obtained ionization potentials for the $A^2\Pi_u(v00)$ levels, the wavelengths for the vibrational transitions, $A^2\Pi_u(v'00) \rightarrow X^2\Pi_g(v''00)$ are calculated and listed in Table IV. As shown in Figure 3 the calculated wavelengths fit the fluorescence spectrum quite well.

C. Production Cross Sections

At a constant primary photon intensity and a constant gas

pressure, the fluorescence cross section, $\sigma_f(\lambda,\lambda_f)$, for a band at wavelength λ_f produced by a primary photon of wavelength λ, is proportional to the fluorescence radiation rate (Lee and Judge, 1972). The relative production cross sections for the various emission wavelengths produced by various incident photon wavelengths are given in Tables I and IV for the $CS_2^+(B^2\Sigma_u^+ \rightarrow X^2\Pi_g)$ and the $CS_2^+(A^2\Pi_u \rightarrow X^2\Pi_g)$ systems, respectively.

The absolute production cross section is obtained by comparing the presently observed fluorescence radiation rates with those of the N_2^+ or CO_2^+ fluorescence, for which the production cross sections are known (Lee and Judge, 1972, Judge and Weissler, 1968). The total production cross sections, $\Sigma_f\sigma_f(\lambda,\lambda_f)$, of the $CS_2^+(A^2\Pi_u, B^2\Sigma_u^+ \rightarrow X^2\Pi_g)$ fluorescence bands produced by incident wavelengths from $\lambda\lambda$462-977 Å are listed in Table V and shown in Figure 4. The absorption cross sections, σ_T, given by Cook and Ogawa (1969) are adopted for the calculation of the production yields, $\eta_f = \sigma_f/\sigma_T$, and are also listed in Table V. The cross sections are in units of Mb ($= 10^{-18}$ cm^2) and the yields in %. The uncertainty for the production cross sections is estimated to be ±15% of the given value.

As shown in Figure 4 the production cross section of the $A^2\Pi_u \rightarrow X^2\Pi_g$ fluorescence at the incident wavelength λ955 Å is exceptionally high. This wavelength is within the strong absorption band (Cook and Ogawa, 1969) associated with the n = 3 member of the Rydberg series III (Tanaka et al., 1960), where a high relative photoionization

cross section is also seen in the ion mass spectrum observed by Dibeler and Walker (1967). Similarly, the large production cross section of the $B^2\Sigma_u^+ \rightarrow X^2\Pi_g$ fluorescence at wavelength λ827 Å is correlated with the strong absorption and ionization (Cook and Ogawa, 1969, Dibeler and Walker, 1967) bands associated with the n = 3 member of the Rydberg series V (Tanaka et al., 1960). For wavelengths shorter than λ800 Å the ion mass spectra (Dibeler and Walker, 1967) show that both the dissociative ionization processes, $CS_2 + h\nu \rightarrow S^+ + CS + e$ and $CS^+ + S + e$, have appreciable efficiencies. Since these dissociative ionization processes will reduce the production of CS_2^+ ions, the cross sections for the production of fluorescence from excited CS_2^+ ions may be expected to decrease at the shorter primary photon wavelengths which are shown in Figure 4.

Acknowledgment

This work was supported by the National Aeronautics and Space Administration under Grant No. NGR 05-018-180.

REFERENCES

Brundle, C. R. and Turner, D. W. 1969. Int. J. Mass Spect. Ion Phys. 2, 195.

Bueso-Sanllehf, Facundo. 1941. Phys. Rev. 60, 556.

Callomon, J. H. 1958. Proc. Roy. Soc. (London). A244, 220.

Collin, J. E. and Natalis, Paul. 1968. Int. J. Mass Spect. Ion Phys. 1, 121.

Cook, G. R. and Ogawa, M. 1969. J. Chem. Phys. 51, 2419.

Diebeler, V. H. and Walker, J. A. 1967. J. Opt. Soc. Am. 57, 1007.

Eland, J.H.D. and Danby, C. J. 1968. Int. J. Mass. Spect. Ion Phys. 1, 111.

Herzberg, G. (Editor). 1966. Electronic spectra of polyatomic molecules (Van Nostrand, N.Y.), p. 150, 601.

Hudson, R. D. 1970. Rev. Geophys. Space Phys. 9, 305.

Johns, J.W.C. 1961. Can. J. Phys. 39, 1738.

Judge, D. L., Bloom, G. S., and Morse, A. L. 1969. Can. J. Phys. 47, 489.

Judge, D. L. and Lee, L. C. 1972. J. Chem. Phys. 57, 455.

Judge, D. L. and Weissler, G. L. 1968. J. Chem. Phys. 48, 4590.

Lee, L. C. and Judge, D. L. 1972. J. Chem. Phys. 57, 4443.

Momigny, J. and Delwiche, J. 1968. J. Chem. Phys. 65, 1213.

Mrozowski, S. 1941. Phys. Rev. 60, 730.

_____ 1942. Phys. Rev. 62, 270.

_____ 1947a. Phys. Rev. 72, 682.

_____ 1947b. Phys. Rev. 72, 691.

Ogawa, M. and Chang, H. C. 1970. Can. J. Phys. 48, 2455.

Price, W. C. and Simpson, D. M. 1932. Proc. Roy Soc. (London). A165, 272.

Slavin, W., Mooney, R. W., and Palumbo, D. T. 1961. J. Opt. Soc. Am. 51, 93.

Tanaka, Y., Jursa, A. S., and LeBlanc, F. J. 1960. J. Chem. Phys. 32, 1205.

Tanaka, Y. and Ogawa, M. 1962. Can. J. Phys. 40, 879.

Turner, D. W. and May, D. P. 1967. J. Chem. Phys. 46, 1156.

Walker, W. C., Wainfan, N., and Weissler, G. L. 1955. J. Appl. Phys. 26, 1366.

Weissler, G. L., Ogawa, M., and Judge, D. L. 1971. J. de Physique Suppl. 32, C4-154.

Table I

The band head positions, the wave numbers, and the relative production cross sections for the various bands of the $CS_2^+(B^2\Sigma_u^+ \rightarrow X^2\Pi_g)$ system produced by photons at various incident wavelengths. The assigned transitions are also given.

band head λ(Å)	Incident λ(Å) / cm^{-1}	835	555 | 827	Transitions $B^2\Sigma_u^+ \rightarrow X^2\Pi_g(\Omega)$
2798	α 35740 *	0.030		(020) → (020) (3/2)
2809	c 35594.83*	0.16		(010) → (010) (3/2)
2820	a 35460.77	1.00	1.00	(000) → (000) (3/2)
2826	35386	0.016		
2834	β 35286 *	0.026		(020) → (020) (1/2)
2844	d 35157.33*	0.13		(010) → (010) (1/2)
2855.5	b 35020.06	0.91	0.86	(000) → (000) (1/2)
2863	34928 *	0.017		
2870	e 34843.95	0.021	0.023	(000) → (100) (3/2)
2874	34795*	0.052	0.055	
2908	f 34389	0.020	0.021	(000) → (100) (1/2)
2914	34317	0.014	0.015	

*The wave numbers are adopted from Callomon

Table II

The ionization potentials for the $A^2\Pi_{u,\Omega}(v00)$ vibrational levels obtained from the presently observed sequence bandheads. The values given by other authors are also given for comparison.

Sequence Band heads $\lambda(\mathring{A})$	Vibrational Levels $^2\Pi_u(V00)(\Omega)$	Ionization Potentials (ev) This Work	Eland and Danby	Bundle and Turner	Ogawa and Chang
4880	0 3/2	12.620	12.634		12.563
4940	1/2	12.643			12.586
4740	1 3/2	12.695	12.704	12.69	12.638
4803	1/2	12.714			12.661
4607	2 3/2	12.770	12.772	12.77	12.711
4671	1/2	12.787			12.735
4497	3 3/2	12.836	12.845	12.84	12.784
4542	1/2	12.863			12.808
4380	4 3/2	12.910	12.917	12.91	12.856
4437	1/2	12.927			12.879

Table III

The wavelengths for the vibrational transitions of the $CS_2^+[A^2\Pi_{u,\Omega}(v'00) \rightarrow X^2\Pi_{g,\Omega}(v''00)]$ system

v' \ v''		0	1	2	3
0	Ω=3/2	4880 Å	5031 Å	5193 Å	5365
	1/2	4940	5099	5268	5450
1	3/2	4740	4883	5035	5196
	1/2	4803	4953	5113	5283
2	3/2	4607	4742	4885	5037
	1/2	4671	4813	4964	5124
3	3/2	4497	4625	4761	4905
	1/2	4542	4676	4818	4969
4	3/2	4380	4500	4630	4766
	1/2	4437	4565	4700	4844

Table IV

The relative cross sections for the $CS_2^+(A^2\Pi_u \rightarrow X^2\Pi_g)$ system in various emission wavelength regions. The $CS_2^+(A^2\Pi_u)$ ions are produced by incident wavelengths of λ923 or 955 Å.

$\Delta\lambda$(Å)	4380 | 4430	4430 | 4475	4475 | 4535	4535 | 4600	4600 | 4650	4650 | 4730	4730 | 4790	4790 | 4875	4875 | 4930	4930 | 5025
σ_f	0.17	0.15	0.43	0.43	0.63	0.75	1.00	0.93	1.07	1.41

λ(Å)	5025 | 5080	5080 | 5180	5180 | 5265	5265 | 5360	5360 | 5570	5570 | 5770
σ_f	1.02	1.44	1.33	1.69	2.32	1.52

Table V

The production cross sections, σ_{Af} and σ_{Bf}, and the yields, η_{Af} and η_{Bf}, respectively for the $CS_2^+(A^2\Pi_u, B^2\Sigma_u^+ \rightarrow X^2\Pi_g)$ fluorescence produced by primary photon wavelengths from λλ462-977Å. The absorption cross sections, σ_T, were given by Cook and Ogawa. The cross sections are in units of Mb(= 10^{-18} cm^2) and the yields $\eta_f(=\sigma_f/\sigma_T)$ are in units of %.

λ(A)	σ_T(Mb)	σ_{Af}(Mb)	η_{Af}(%)	σ_{Bf}(Mb)	η_{Bf}(%)
462		2.3		1.5	
501		3.4		2.0	
526		3.9		3.6	
555		4.5		5.0	
589		4.7		7.5	
598		4.9		6.6	
610	35.7	4.8	13	6.2	17
625	36.2	4.6	13	5.2	14
637	37.8	5.1	13	6.1	16
645	38.1	4.8	13	5.9	15
689	45.1	4.9	11	9.5	21
702	44.8	5.7	13	10.8	24
716	46.3	6.3	14	9.7	21
731	46.5	6.9	15	6.9	15
769	48.0	8.3	17	8.9	19
772	49.5	8.8	18		
790	68.5	9.7	14	16.4	24
801	60.7	10.4	17	17.5	29
809	45.8			6.6	14
815	57.7			10.3	18
822	45.8			19.6	43
827	82.0	11.6	14	56.0	68
835	77.4	10.1	13	37.3	48
840	37.2			15.9	43
844	37.2	7.0	19	16.7	45
851	27.9	5.7	20	8.8	31
879	52.1	7.9	15		
894	43.2	7.6	18		
901	83.6	14.2	17		
923	45.4	30.2	67		
955	120.2	64.9	54		
977		1.7			

Figure Captions

Fig. 1 The fluorescence spectra of the $CS_2^+[B^2\Sigma_u^+ \rightarrow X^2\Pi_g]$ system produced by primary photons of wavelengths λ555, 827, 835 and 851 Å.

Fig. 2 The fluorescence spectrum of the $CS_2^+[B^2\Sigma_u^+ \rightarrow X^2\Pi_g]$ system produced by primary photons of wavelength λ835 Å. The band heads, a-y, given by Callomon are indicated. The suggested assignments for the α,c,β, and d bands are also indicated.

Fig. 3 The fluorescence spectrum of the $CS_2^+[A^2\Pi_u \rightarrow X^2\Pi_g]$ system produced by primary photons of wavelength λ923 Å. The suggested assignments for the observed bands are indicated.

Fig. 4 The production cross sections of the $CS_2^+[A^2\Pi_u \rightarrow X^2\Pi_g]$ and $CS_2^+[B^2\Sigma_u^+ \rightarrow X^2\Pi_g]$ fluorescence which are indicated by $\cdot$ and $\dot{x}$, respectively. The units are in Mb(= 10^{-18} cm^2).

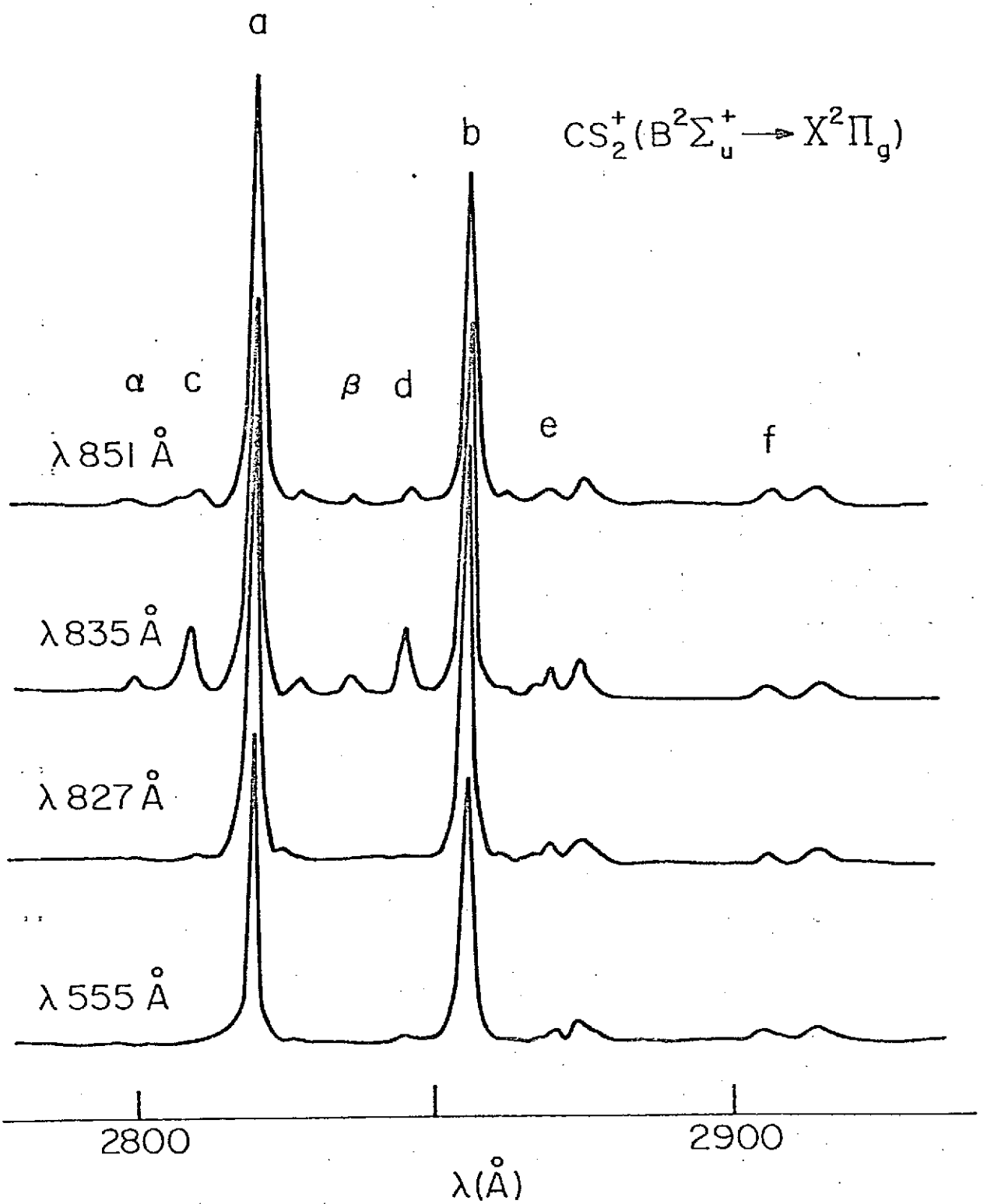
a
b
$CS_2^+(B^2\Sigma_u^+ \rightarrow X^2\Pi_g)$
α
c
β
d
e
f
λ 851 Å
λ 835 Å
λ 827 Å
λ 555 Å
2800
2900
λ(Å)

27

Fig. 1

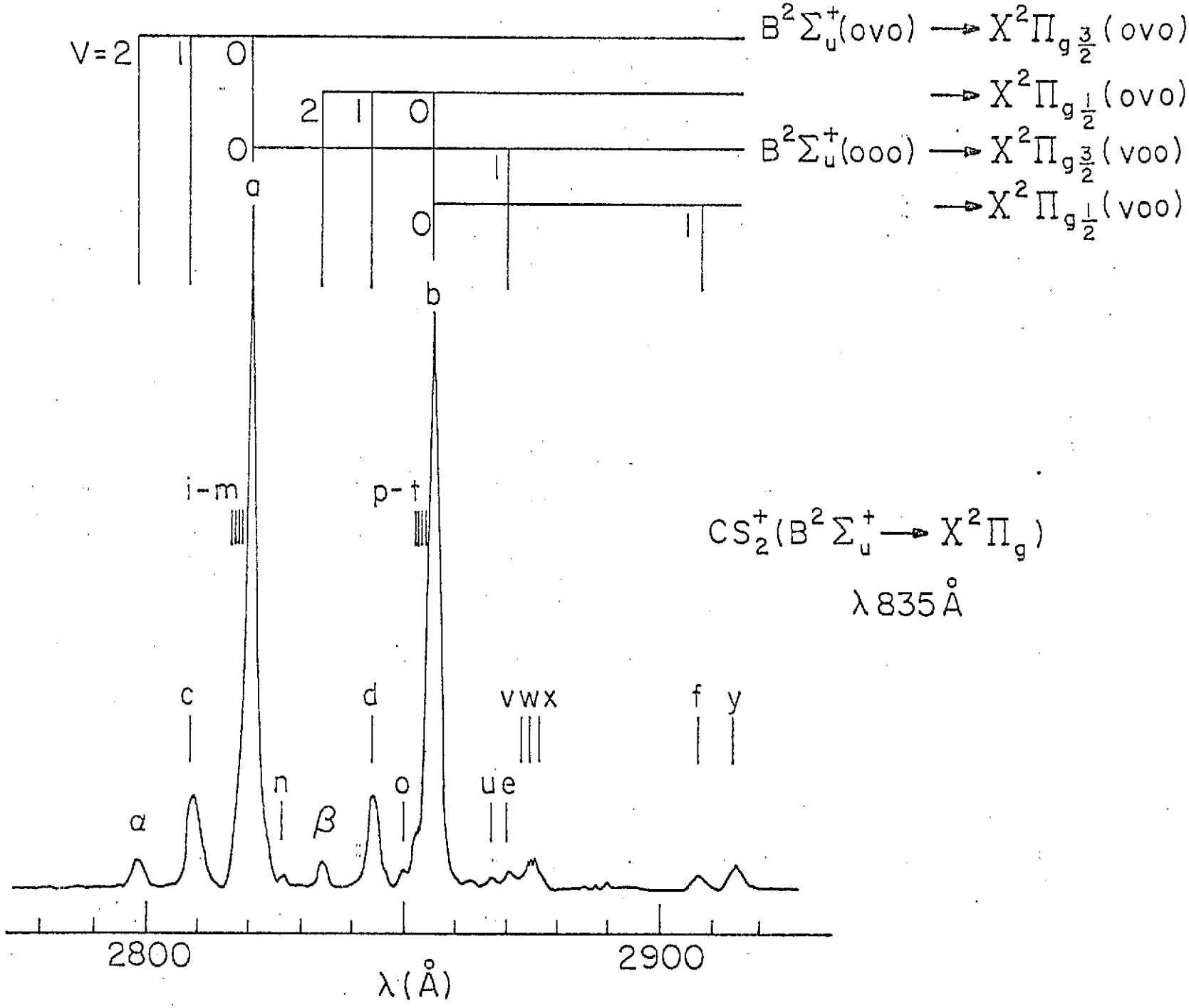
V=2
1
0
0
2
1
0
0
1
0
1
a
b
$B^2\Sigma_u^+(ovo) \rightarrow X^2\Pi_{g\frac{3}{2}}(ovo)$
$\rightarrow X^2\Pi_{g\frac{1}{2}}(ovo)$
$B^2\Sigma_u^+(ooo) \rightarrow X^2\Pi_{g\frac{3}{2}}(voo)$
$\rightarrow X^2\Pi_{g\frac{1}{2}}(voo)$
i-m
p-t
$CS_2^+(B^2\Sigma_u^+ \rightarrow X^2\Pi_g)$
λ835 Å
c
d
vwx
f
y
α
n
β
o
ue
2800
2900
λ(Å)

Figure 2

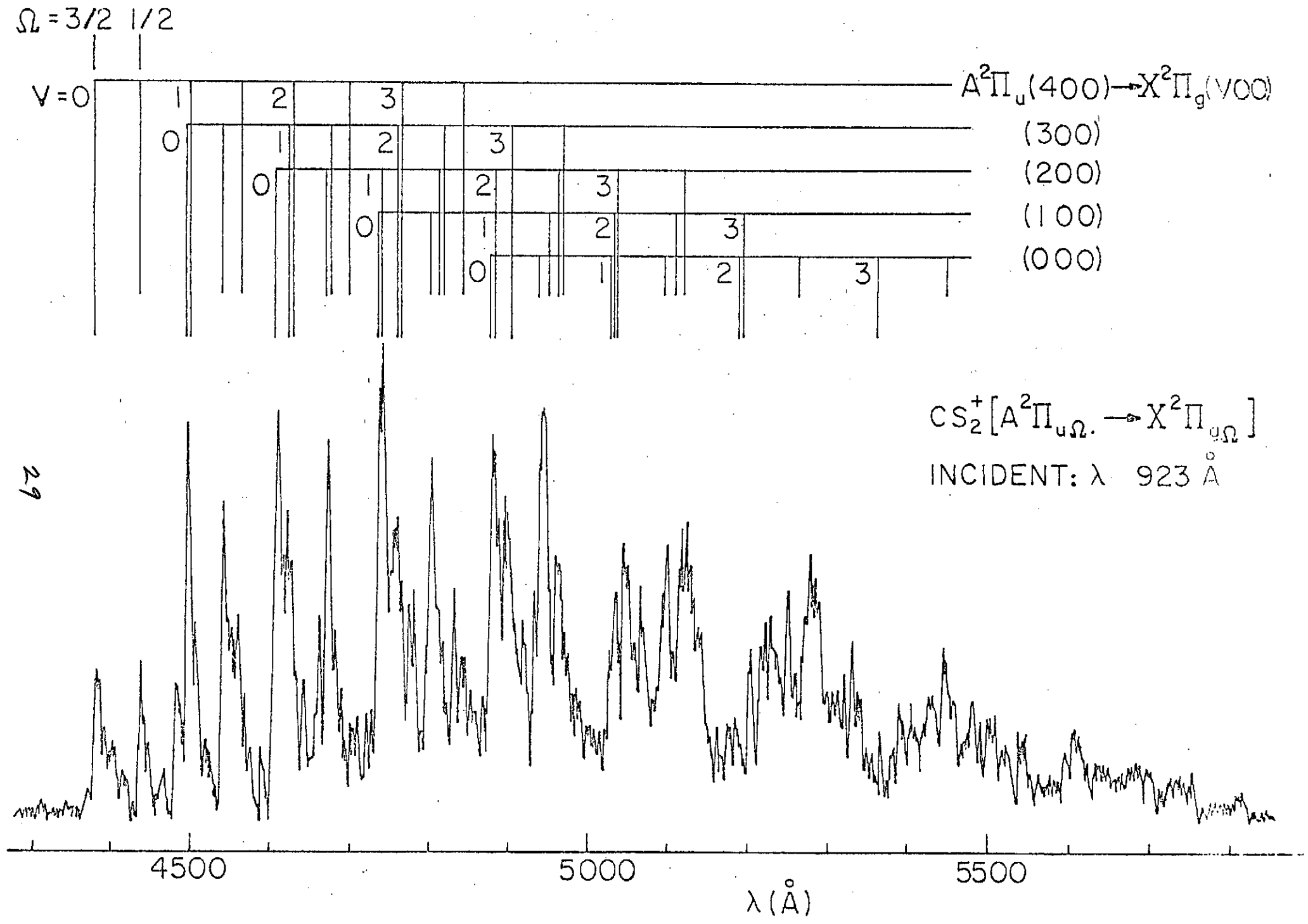
Ω = 3/2 1/2
V = 0
A²Π_u(400)→X²Π_g(V00)
(300)
(200)
(100)
(000)
CS₂⁺[A²Π_uΩ. → X²Π_gΩ]
INCIDENT: λ 923 Å
29
4500
5000
5500
λ(Å)

Fig. 3

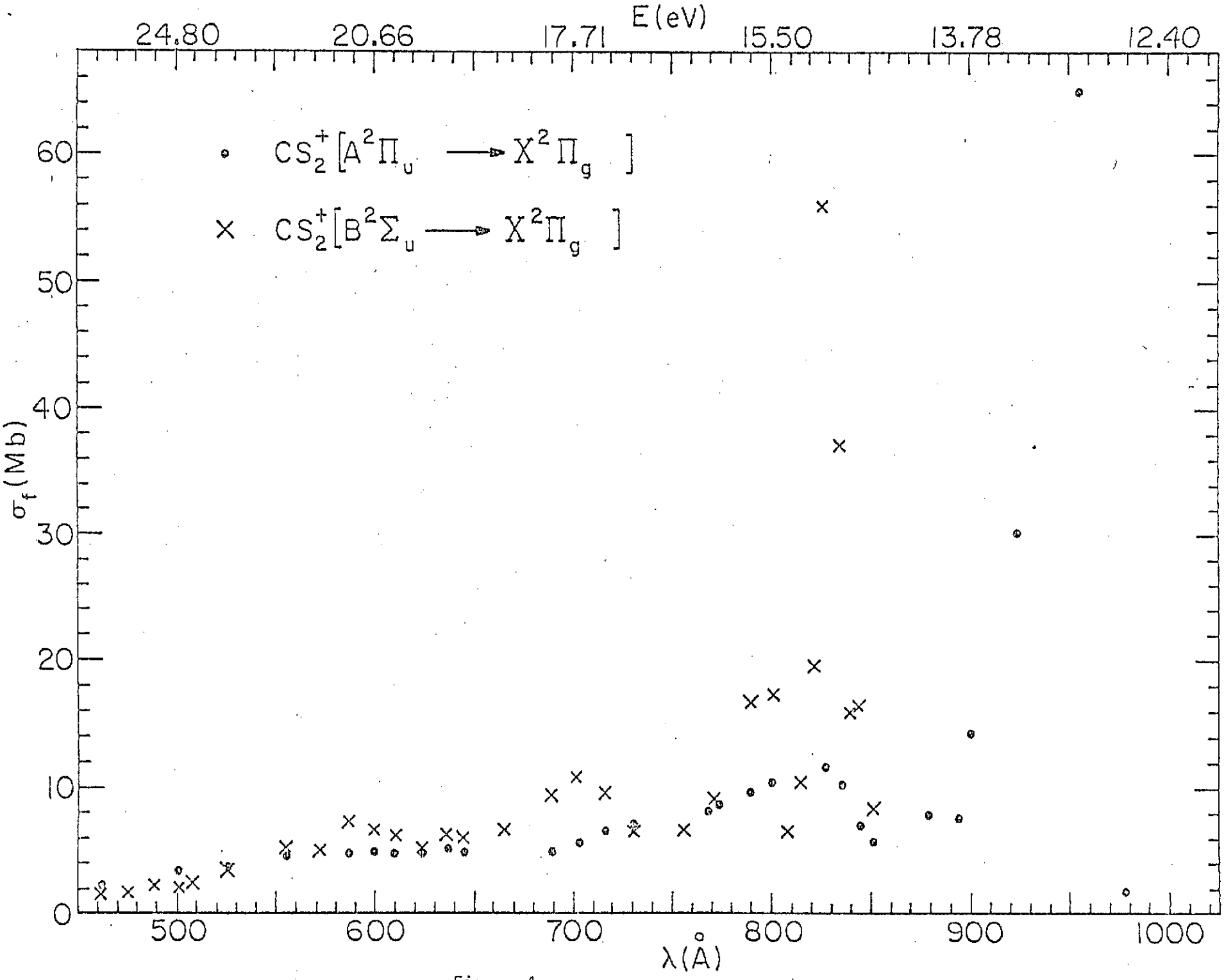
E(eV)
24.80
20.66
17.71
15.50
13.78
12.40
$CS_2^+[A^2\Pi_u \longrightarrow X^2\Pi_g]$
$CS_2^+[B^2\Sigma_u \longrightarrow X^2\Pi_g]$
σ_f(Mb)
0
10
20
30
40
50
60
500
600
700
800
900
1000
λ(Å)

Figure 4

$CS(A^1\Pi \rightarrow X^1\Sigma^+)$ FLUORESCENCE FROM PHOTODISSOCIATION OF CS_2 AND OCS

L. C. Lee and D. L. Judge

Department of Physics
University of Southern California
Los Angeles, California 90007

Abstract

The $CS(A^1\Pi \rightarrow X^1\Sigma^+)$ fluorescence resulting from photodissociation of CS_2 and OCS by vacuum ultraviolet emission lines from λλ686-1239 Å has been investigated. With the assumption that the electronic transition moment is constant, the Franck-Condon factors for the emission system and the population in the vibrational levels of the $CS(A^1\Pi)$ electronic state have been measured. The population data are approximately represented by a Poisson distribution, which is predicted from a theoretical argument. A population inversion between the $v = 0$ and 1 levels of the $CS(A^1\Pi)$ state is found. The production cross sections for the fluorescence are also measured.

I. INTRODUCTION

The $CS(A^1\Pi \rightarrow X^1\Sigma^+)$ fluorescence produced by photodissociative excitation of CS_2 produced by photons in the wavelength range from λλ1200-1337 Å has been observed by Okabe[1]. The excited photofragment $CS(A^1\Pi)$ is mainly produced by the process

$$CS_2 + h\nu \rightarrow CS(A^1\Pi) + S(^3P_2)$$

The ultraviolet fluorescence at wavelengths shorter than λ4500 Å, produced by OCS absorbing photons of wavelengths from λλ650-1000 Å, has been reported by Cook and Ogawa[2]. However, the source of the fluorescence was not identified.

The fluorescence spectra from photofragments provide data required for an understanding of photodissociation mechanisms. Recently, several theoretical arguments[3-6] have predicted the population distribution in the vibrational levels of a diatomic photofragment. Such theoretical predictions can be investigated by observing the fluorescence spectra as has been demonstrated in earlier work[7] and again in the present investigation.

II. EXPERIMENTAL

The experimental setup has been described in a previous paper[8]. The nominal vacuum UV emission lines selected for this investigation were 686, 765, 790, 834, 923, 955, 977, 992, 1037, 1085, and 1239 Å. The bandwidth of the 1-m normal incidence monochromator used for isolation of these lines was set at 5 Å or less. The absolute line intensities were measured with a nickel film photoelectric detector for which the quantum efficiency was known[9]. The fluorescence was dispersed by either of two gratings, one blazed at 2000Å and the other at 5000 Å, of which the first and the second orders were used, respectively. The bandwidth of the 0.3-m normal incidence monochromator used in the present investigations was set at 3 Å or less.

The combined response of the 0.3-m monochromator and cooled photomultiplier (EMI 9558 QB) was calibrated against the response of sodium salicylate, of which the fluorescent efficiency between 2200 and 3400 Å is known to be constant[10]. The spectral region of interest extends from λλ2400-2900 Å and throughout this range the detection system response (per photon/second) is found to be nearly constant.

CS_2 vapor was obtained from an analytical-reagent-grade liquid. The vapor was purified so that the fluorescence from the possible impurities, especially N_2, produced by vacuum ultraviolet radiation of λ555 Å was not detectable. OCS gas supplied by Matheson Gas Co. with a purity higher than 97.5% was used without further purification. The gas pressure inside the sample cell was monitored with a Baratron capacitance manometer and was limited to 20 mtorr or less where the fluorescence intensity is linearly proportional to the pressure.

III. RESULTS AND DISCUSSION

A. Fluorescence Spectra

The $CS(A^1\Pi \rightarrow X^1\Sigma^+)$ fluorescence produced by photodissociation of CS_2 with primary photons of wavelength λ1239 Å is shown in Fig. 1. The radiation was dispersed and the second order spectrum was identified through the bandhead positions given by Pearse and Gaydon[11]. For primary photons of wavelength λ923 Å the same CS fluorescence spectrum was produced by photodissociation of CS_2 and OCS. The resulting first order spectra may be seen in Fig. 2. At λ923 Å the advantage of using the second order to obtain higher resolution is obscured by the emissions from CS_2^+, OCS^+ ions and/or other photofragments. Several spectra were taken at various primary photon wavelengths shorter than λ1239 Å for CS_2 and shorter than λ992 Å for OCS. These spectra are not significantly different from the spectra shown in Figures 1 and 2. According to the photodissociation energy of CS_2(= 4.463 eV) given by Okabe,[1] fluorescence emitted from levels higher than $v' = 5$ of $CS(A^1\Pi)$ is energetically possible for primary photon wavelengths shorter than λ1239 Å. However, the fluorescence from these higher vibrational levels is rather weak.

B. Franck-Condon Factors of the $CS(A^1\Pi \rightarrow X^1\Sigma^+)$ System

The fluorescence radiation rate, $\dot{n}_{v'v''}$, for a band emitted from a vibrational level v' of the upper electronic state to a level v" of the lower electronic state can be obtained from the measured spectra. Because of the constancy of the detection system response the relative radiation rate for each emission is proportional to the area under its spectral envelope. The radiation rates for various emission bands resulting from CS_2 and OCS absorbing various primary photon wavelengths are listed in Table I. These values are averaged over several spectra obtained under similar

conditions and in which the (1-1) band of each spectrum is normalized to 1.

The radiation rate[12] has been given by

$$\dot{n}_{v'v''} = KN_{v'} Re^2_{v'v''} q_{v'v''} / \lambda^3_{v'v''}$$

where K is a constant, $N_{v'}$ is the population in the vibrational level v', $Re_{v'v''}$ is the electronic transition moment, $q_{v'v''}$ is the Franck-Condon Factor, and $\lambda_{v'v''}$ is the band wavelength.

If the electronic transition moment is assumed to be a constant, which is usually a good assumption for diatomic molecules[8], then the Franck-Condon factor can be calculated from the measured radiation rates and the known band wavelengths[11]. The Franck-Condon factors obtained from the spectra resulting from CS_2 absorbing photons of wavelength $\lambda 1239\mathring{A}$ are listed in Table I. The sum of the Franck-Condon factors over the lower level v", $\Sigma\, q_{v'v''}$, for each upper level is equal to 1. The calculated Franck-Condon factors given by Felenbok[13] are also listed for comparison. In general, except for the $\Delta v = o$ transitions, the measured values agree with the theoretical values. This agreement strengthens the validity of a constant electronic transition moment.

C. Population Distribution of the $CS(A^1\Pi)$ levels

If the electronic transition moment is assumed to be constant, the population $N_{v'}$ in an upper level, v', can be obtained from

$$N_{v'} = K' \sum_{v''} \dot{n}_{v'v''} \lambda^3_{v'v''}$$

The population distributions in the vibrational levels of $CS(A^1\Pi)$ produced by photodissociation of CS_2 with primary photon wavelengths of $\lambda 923$ and $\lambda 1239$ Å and OCS with $\lambda 923$ Å are shown in Fig. 3 and 4, respectively. The population in the v' = 1 level is normalized to 1. The error bar shows the fluctuation of data obtained from various spectra.

A population inversion between the $v = 0$ and 1 levels is evident.

The photodissociation mechanism has been summarized and generalized by Simons and Tasker[3]. When a CS_2 or OCS molecule absorbs a photon it is excited to a repulsive state and the molecular CS fragments will occupy a range of initial vibrational states determined by the appropriate Franck-Condon factors. During the separation period the CS fragments are then forced into a set of final states by the recoil force. If we assume that the vibrational state of CS is that of a harmonic oscillator, and the recoil force corresponds to an exponentially repulsive potential, then the probability that $CS(A^1\Pi)$ in an initial state i will be transferred to a final vibrational level v' is given by [4,14-16]

$$P_{v'i} = i!\, v'!\, (\Delta E)^{i+v'}\, e^{-\Delta E} \left[\sum_{\ell=0}^{\min(i,v')} \frac{(-\Delta E)^{-\ell}}{\ell!(i-\ell)!\,(v'-\ell)!}\right]^2$$

where ΔE is the average number of vibrational quanta transferred.

If we assume that the initial states are only prepared in the ground state, i = o, then the population, $N_{v'}$, is a Poisson distribution,

$$N_{v'} \propto P_{v'o} = (\Delta E)^{v'}\, e^{-\Delta E}/v'!$$

The Poisson distribution best fit to the measured populations is shown in Figs. 3 and 4. The ΔE values for CS_2 dissociated by photons of wavelengths λ1239 and 923 Å, and for OCS by λ923 Å, are 1.66, 1.86, and 1.82, respectively.

As indicated in the figures the measured populations are only approximately represented by the Poisson distribution. It seems that the initial states are also prepared in higher excitation states. If we assume that both the i = o and 1 states are initially populated and that the number of vibrational quanta transferred is the same for both states, then the population in the vibrational level v' is given by

$$N_{v'} = N_1\, (\Delta E)^{v'-1}[(\Delta E)^2 + (\alpha - 2v')\,\Delta E + v'^2]/\{v'![(\Delta E)^2+(\alpha-2)\,\Delta E+1]\}$$

where α is the ratio of the population in the i= state to that in the i=1 state.

The result for the best fit of the observed populations using the above equation is shown in Figs. 3 and 4. The values of ΔE and α for the observed distributions are 1.665 and 12.60 for CS_2 photodissociated by photons of wavelength λ1239 Å, 1.951 and 4.48 for CS_2 photodissociated by λ923 Å, and 1.914 and 4.25 for OCS dissociated by λ923 Å. A comparison of the ΔE and α values of CS_2 dissociated by λ1239 Å with those by λ923 Å indicates that as the primary photon energy is increased more vibrational quanta are transferred and that the initial states include higher vibrational levels.

As indicated in the figures the measured populations are only approximately represented by the theoretical distribution modified to involve the initial state i=1. The initial populations in the other higher excited states and the anharmonicity of the $CS(A^1\Pi)$ potential well should be considered. On the other hand, Berry[17] and Band and Freed[18] have proposed different photodissociation models in which the interfragment force during the separation period is ignored and the final population distribution is solely determined by the initial Franck-Condon factors and the continua state densities. Such models may provide an alternative interpretation for the present measurements.

D. Production Cross Sections of the Fluorescence

At low gas pressure, P, the radiation rate produced by a primary photon of wavelength λ is proportional to the production cross section $\sigma_{v'v''}(\lambda)$ and is given by[19]

$$\dot{n}_{v'v''}(\lambda) = K\, \sigma_{v'v''}(\lambda)\, I_o\, (\lambda)\, P$$

where K is a constant and $I_o(\lambda)$ is the primary photon flux.

The absolute total cross section, $\sum_{v'v''} \sigma_{v'v''}(\lambda)$, at each primary wavelength is obtained by comparing the total fluorescence radiation $\sum_{v'v''} \dot{n}_{v'v''}$, with that of the CO^+ first negative band, for which the absolute cross section is known[8]. The cross sections for the $CS(A^1\Pi \rightarrow X^1\Sigma^+)$ fluorescence produced by photodissociation of CS_2 and OCS, at various primary photon wavelengths, are listed in TableII. The fluorescence production cross sections for the primary photon wavelengths from λ462 to 686 Å are estimated to be smaller than 0.02 Mb for both CS_2 and OCS.

E. The D(O - CS) Dissociation Energy

The threshold for the production of the $CS(A^1\Pi \rightarrow X^1\Sigma^+)$ fluorescence from photodissociation of CS_2 as measured by Okabe[1] is 1337 ± 2 Å. On the other hand, the threshold for the production of fluorescence from photodissociation of OCS has not been given. In the present measurement weak fluorescence has been observed at the primary photon wavelength of λ1010 Å and no detectable fluorescence signal has been produced by λ1037 Å photons. Therefore, the threshold for the production of $CS(A^1\Pi)$ fragments from photodissociation of OCS is 1024 ± 14 Å or 12.11 ± 0.16 eV. If we assume that the photodissociation is through the following process

$$OCS + h\nu \rightarrow CS(A^1\Pi) + O(^3P) \qquad (1)$$

which is spin forbidden, but corresponds to the CS_2 photodissociation process at threshold[1], the photodissociation energy D_0° (O - CS) is then found to be 7.30 ± 0.16 eV or 168 ± 3.7 KCal/mol, subtracting the 4.814 eV (λ2575.6Å) energy of the $CS(A^1\Pi, v'=o) \rightarrow CS(X^1\Sigma^+, v''=o)$ transition from the primary photon energy.

The presently obtained dissociation energy is comparable to that calculated from thermochemical data. Using $\Delta H^\circ_{f,o}(O) = 58.983$ and $\Delta H^\circ_{f,o}(OCS) = -33.991$ Kcal/mol given by Wagman et al.[20] and $\Delta H^\circ_{f,o}(CS) = 64.96 \pm 0.4$ Kcal/mol

derived from the photodissociation threshold of CS_2 given by Okabe,[1] the dissociation energy is

$$D_o^\circ (O - CS) = \Delta H_{f,o}^\circ(CS) - \Delta H_{f,o}^\circ(OCS) + \Delta H_{f,o}^\circ(O)$$
$$= 157.93 \text{ Kcal/mol}$$

This value is about 10 Kcal/mol lower than the presently measured value of 168 ± 3.7 Kcal/mol. However, these closely related values show that the process (1) is the main primary process at threshold. If we assume that the spin allowed process

$$OCS + h\nu \rightarrow CS\ (A^1\Pi) + O\ (^1D) \qquad (2)$$

is the primary process, then the photodissociation energy D_o° (O - CS) will be lowered by the 1.967 eV excitation energy of $O(^1D)$, and accordingly D_o° (O - CS) would be 5.33 ± 0.16 eV or, 123 ± 3.7 Kcal/mol. This value is much lower than that of 157.93 Kcal/mol and therefore, process (2) occurring at the photodissociation threshold is very unlikely.

Acknowledgments

The authors wish to thank Drs. Berry, Band, and Freed for the preprints describing their proposed photodissociation models. This work was supported by the National Aeronautics and Space Administration under Grant No. NGR 05-018-180.

REFERENCES

1. Hideo Okabe, J. Chem. Phys. 56, 4381 (1972).
2. G.R. Cook and M. Ogawa, J. Chem. Phys. 51, 647 (1969)
3. J.P. Simons and P.W. Tasker, Mol. Phys. 26, 1267 (1973)
4. K.E. Holdy, L.C. Klotz, and K.R. Wilson, J. Chem. Phys 52, 4588 (1970)
5. M. Shapiro and R. D. Levine, Chem. Phys. Lett. 5, 499 (1970)
6. Shaul Mukamel and Joshua Jortner, J. Chem. Phys. 60, 4760 (1974)
7. L.C. Lee and D. L. Judge, Can. J. Phys. 51, 378 (1973)
8. D.L. Judge and L.C. Lee, J. Chem Phys. 57, 455 (1972)
9. W.C. Walker, N. Wainfain, and G.L. Weissler, J. Appl. Phys. 26, 1366 (1955)
10. J.A.R. Samson, "Techniques of Vacuum Ultraviolet Spectroscopy" (Wiley, New York, 1967) P. 212
11. R.W. B. Pearse and A. G. Gaydon, "The Identification of Molecular Spectra," (Wiley, New York 1963), P. 125
12. G. Herzberg, "I. Spectra of Diatomic Molecules," (Van Nostrand, New Jersey 1967) P. 200
13. F. Felenbok, Proc. Phys. Soc. 86, 676 (1965)
14. E.H. Kerner, Can. J. Phys. 36, 371 (1958)
15. F.E. Heidrich, K.R. Wilson, and Donald Rapp, J. Chem. Phys. 54, 3885 (1971)
16. D. Rapp and T. Kassal, Chem. Rev. 69, 61 (1969)
17. M. J. Berry, Chem. Phys. Lett. 29, 329 (1974).
18. Y. B. Band and K. F. Freed, Chem. Phys. Lett. 28, 328 (1974).
19. D. L. Judge and L. C. Lee, J. Chem. Phys. 58, 104 (1973)
20. D.D. Wagman, W.H. Evans, V.B. Parker, I. Halow, S. M. Bailey and R.H. Schumm, Natl. Bur. Std. Tech. Note 270-3 (1968)

TABLE I

The radiation rates, $\dot{n}_{v'v''}$, and the Franck-Condon factors, $q_{v'v''}$, for the various bands of the CS($A^1\Pi \rightarrow X^1\Sigma^+$) system produced by photodissociation of CS_2 and OCS.

Molecules / Incident λ		CS_2 1239 Å			CS_2 923 Å	OCS 923 Å
Bands v'-v"	Bandheads $\lambda_{v'v''}$(Å)	$\dot{n}_{v'v''}$	$q_{v'v''}$	Calc. $q_{v'v''}$	$\dot{n}_{v'v''}$	$\dot{n}_{v'v''}$
0-0	2575.6	0.80	0.78	0.7747	0.67	0.73
0-1	2662.6	0.14	0.15	0.1937	0.09	0.11
0-2	2754.7	0.05	0.06	0.0283		
1-0	2507.3	0.24	0.13	0.1968	0.22	0.25
1-1	2589.6	1.00	0.61	0.4040	1.00	1.00
1-2	2677.0	0.31	0.20	0.3044	0.19	0.24
1-3	2769.2	0.07	0.05	0.0798		
2-0	2444.8	0.04	0.03	0.0260		
2-1	2523.2	0.32	0.25	0.3139	0.34	0.29
2-2	2605.9	0.44	0.37	0.1506	0.39	0.42
2-3	2693.2	0.31	0.29	0.3273	0.29	0.32
2-4	2785.7	0.06	0.06	0.1420		
3-1	2460.2	0.07	0.08	0.0764		
3-2	2538.7	0.27	0.33	0.3416	0.38	0.36
3-3	2621.6	0.12	0.16	0.0230	0.16	0.21
3-4	2708.9	0.21	0.31	0.2764	0.26	0.26
3-5	2801.5	0.09	0.14	0.1973		
4-2	2477.0	0.08	0.12	0.1404	0.10	0.10
4-3	2555.8	0.33	0.52	0.2912	0.40	0.42
4-4	2638.9	0.04	0.06	0.0034		
4-5	2726.7	0.15	0.29	0.1822	0.19	0.19

TABLE II

Cross sections for the $CS(A^1\Pi \rightarrow X^1\Sigma^+)$ fluorescence produced by photodissociation of CS_2 and OCS. The cross sections and the primary photon wavelengths are in units of Mb(= 10^{-18} cm^2) and Å, respectively.

λ(Å)	CS_2	OCS
686		0.03
765		0.04
790	0.02	0.08
834	0.04	0.09
923	0.28	0.24
955	0.18	0.21
977	0.17	0.29
992	0.24	0.28
1037	0.52	0
1085	0.39	0
1239	1.09	0

FIGURE CAPTIONS

Fig. 1. The $CS(A^1\Pi \rightarrow X^1\Sigma^+)$ fluorescence spectrum produced by photodissociation of CS_2 with primary photon wavelength of λ1239 Å. The bandhead positions given by Pearse and Gaydon are indicated.

Fig. 2. The $CS(A^1\Pi \rightarrow X^1\Sigma^+)$ fluorescence spectra produced by photodissociation of OCS and CS_2 with primary photon wavelength of λ923 Å.

Fig. 3. The vibrational population of the $CS(A^1\Pi)$ state produced by photodissociation of CS_2 with primary photon wavelengths of λ923 and 1239 Å. Both the best fit Poisson and modified distributions are indicated. The modified distribution has the initial population in both the $v = 0$ and 1 levels.

Fig. 4. The vibrational population of the $CS(A^1\Pi)$ state produced by photodissociation of OCS with primary photon wavelength of λ923 Å. Both the best fit Poisson and modified distributions are indicated.

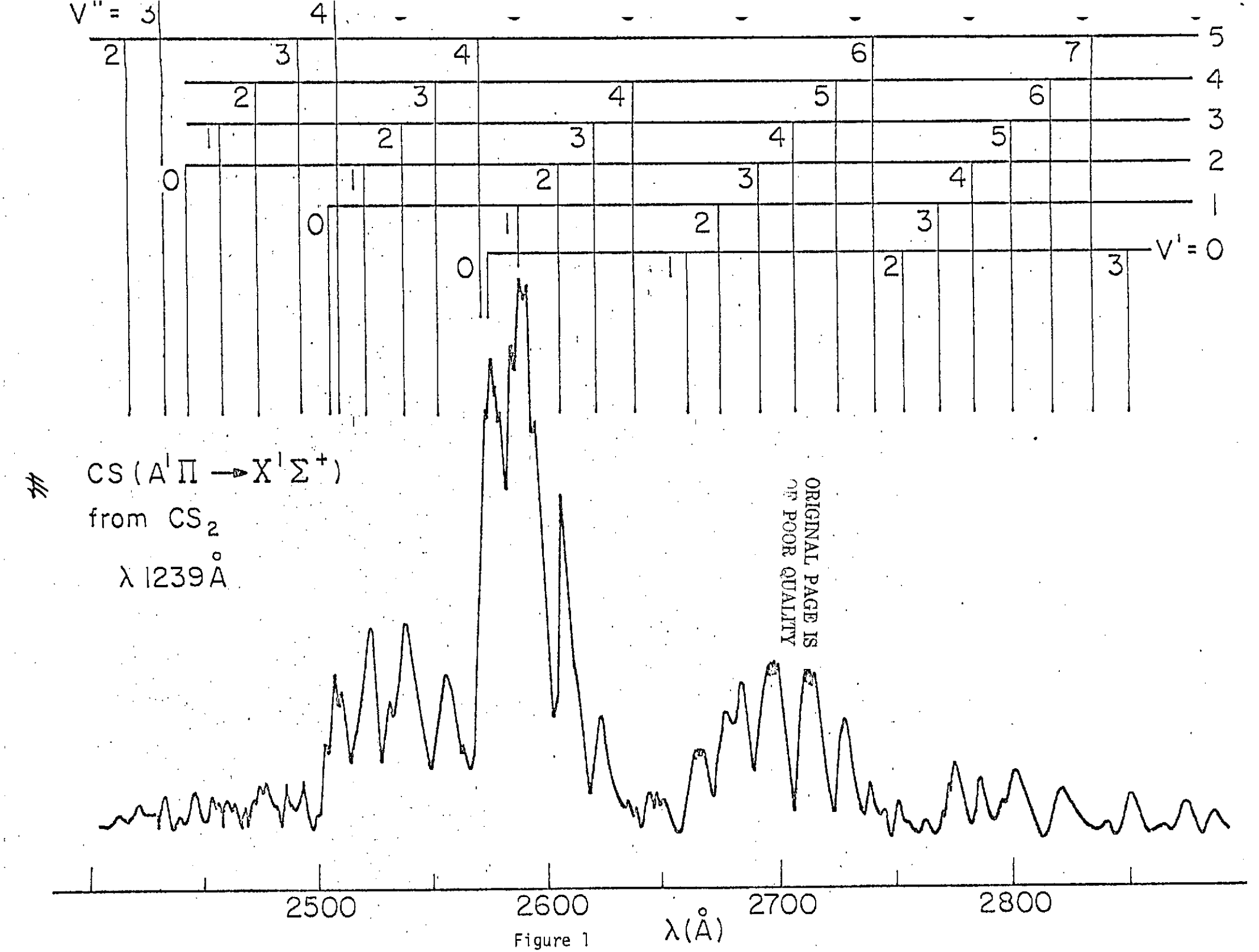

Figure 1

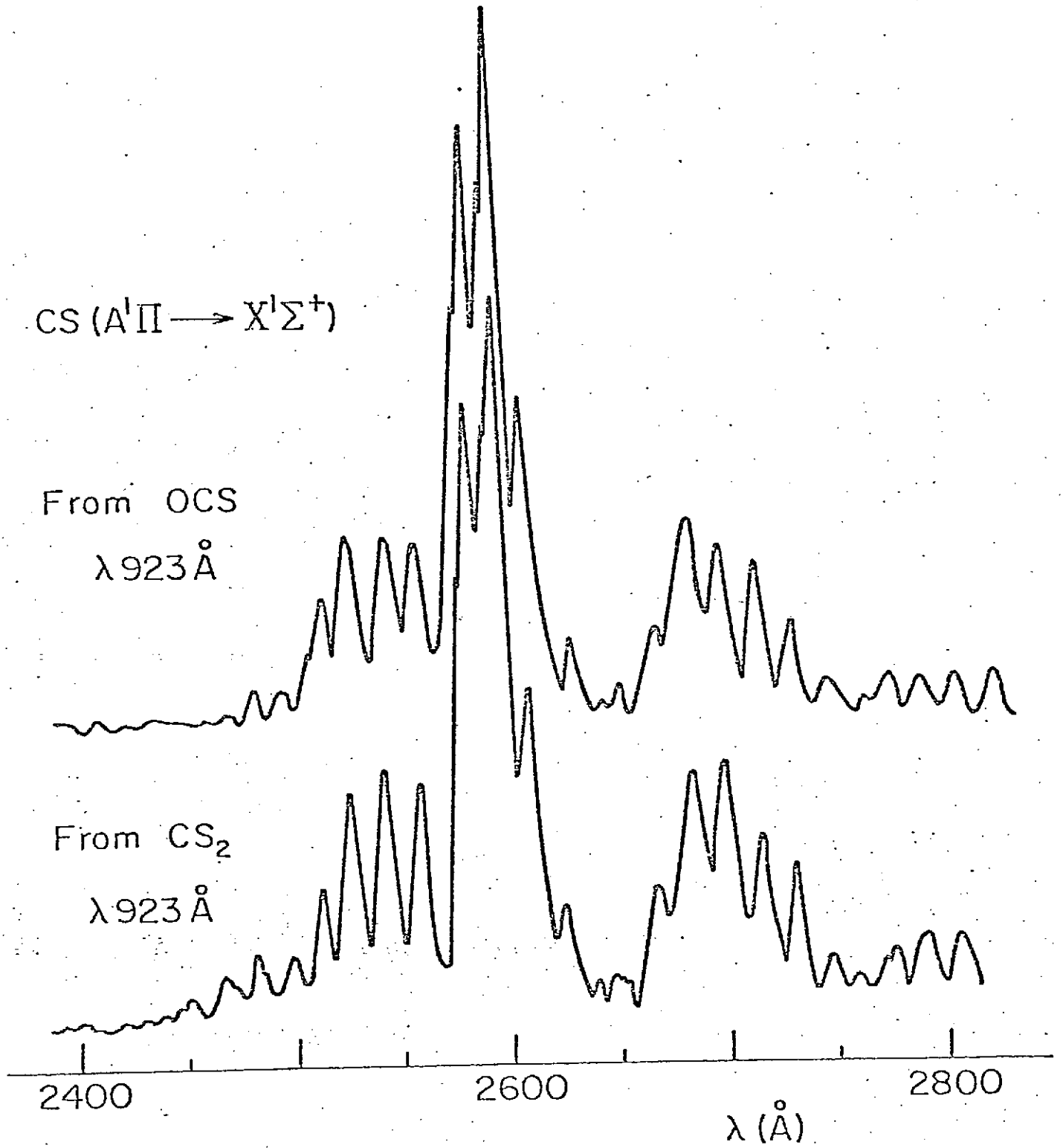

Figure 2

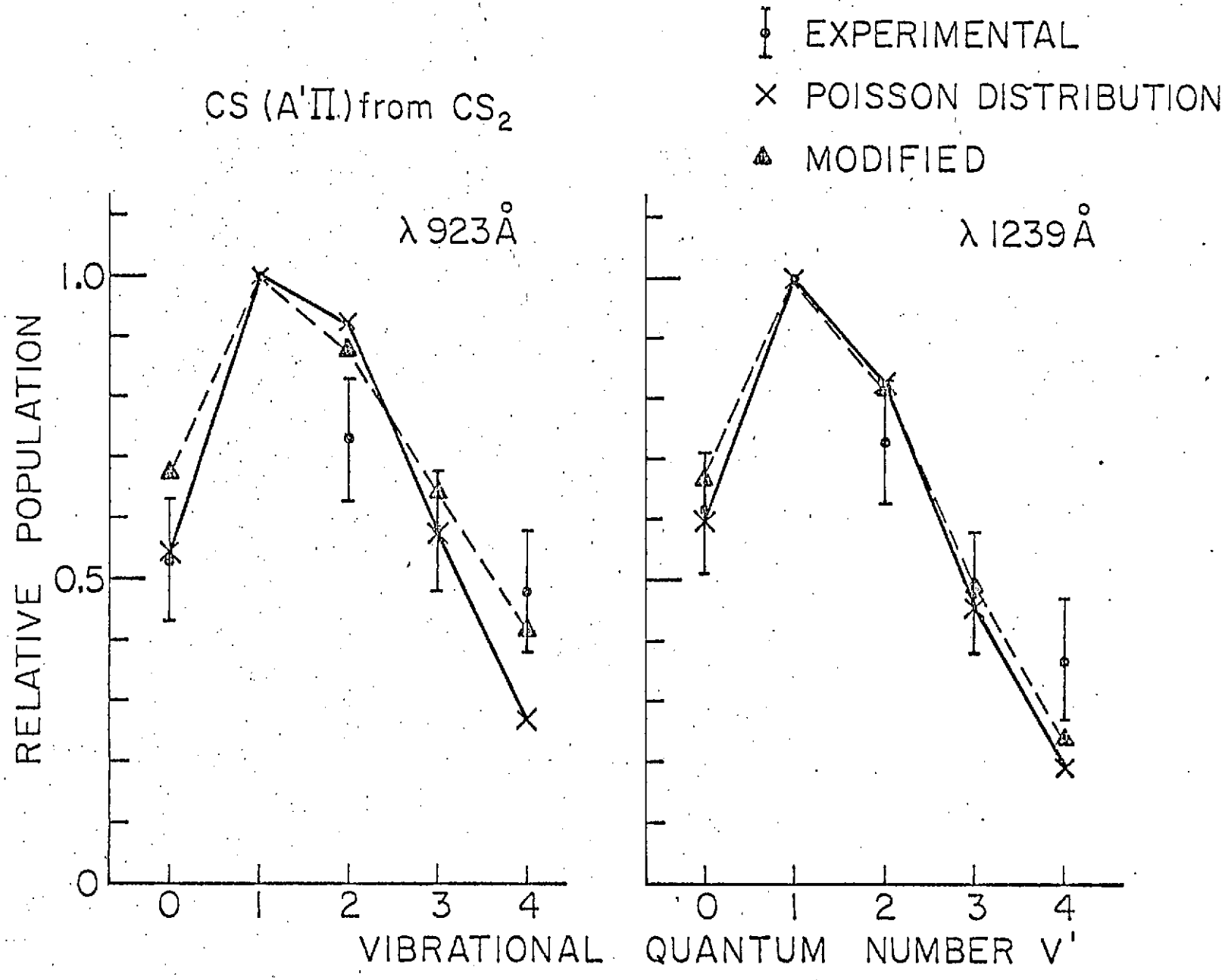
CS (A'Π) from CS_2
EXPERIMENTAL
POISSON DISTRIBUTION
MODIFIED
λ 923Å
λ 1239Å
RELATIVE POPULATION
1.0
0.5
0
0 1 2 3 4
VIBRATIONAL QUANTUM NUMBER V'
0 1 2 3 4

Figure 3

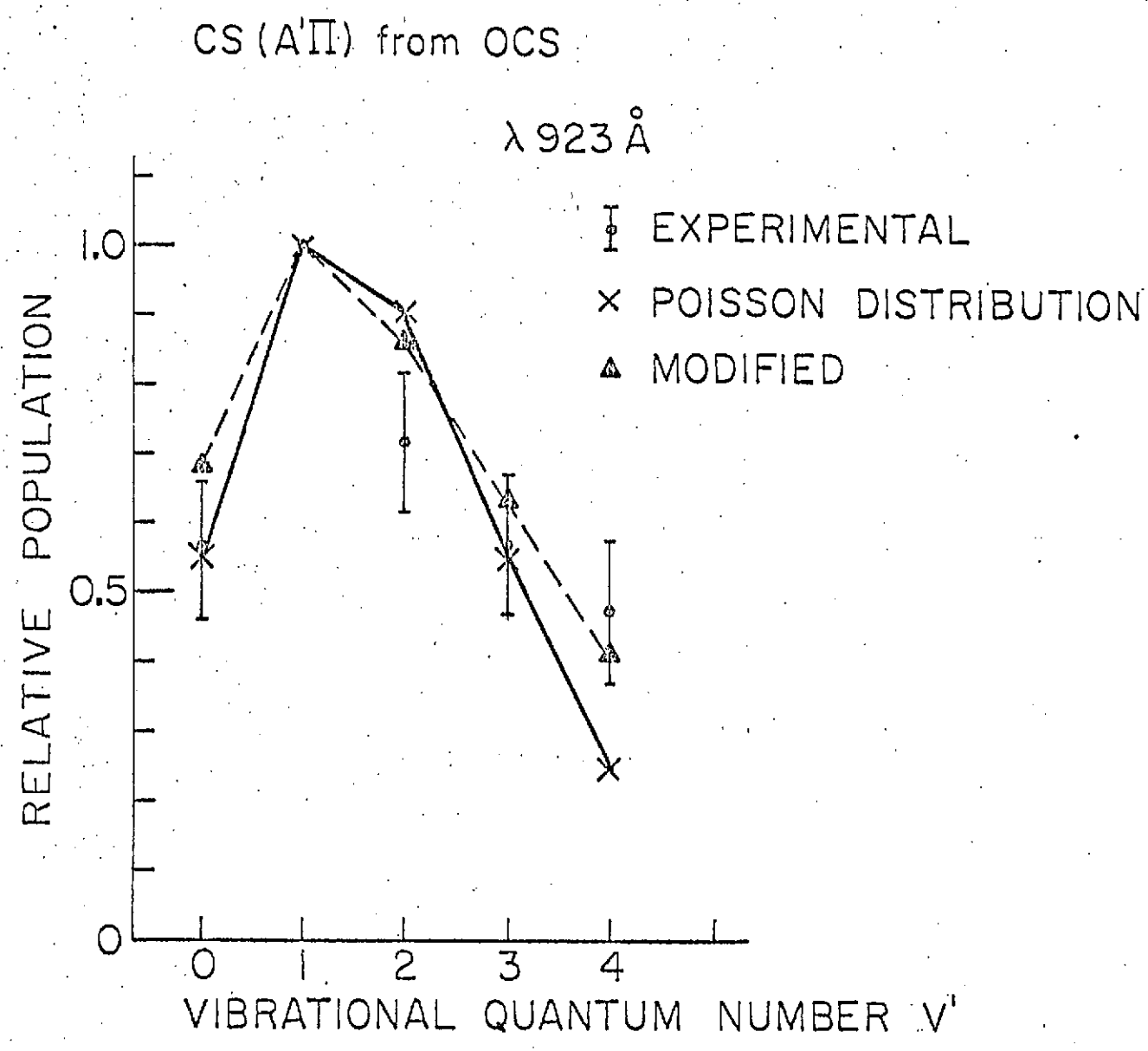
CS (A'Π) from OCS
λ 923 Å
EXPERIMENTAL
POISSON DISTRIBUTION
MODIFIED
RELATIVE POPULATION
1.0
0.5
0
0
1
2
3
4
VIBRATIONAL QUANTUM NUMBER V'

Figure 4

$OCS^+(A^2\Pi \rightarrow X^2\Pi)$ FLUORESCENCE FROM PHOTOIONIZATION OF OCS

D. L. Judge and L. C. Lee

Department of Physics
University of Southern California
Los Angeles, California 90007

Abstract

$OCS^+[A^2\Pi(000) \rightarrow X^2\Pi(v_1 0 v_3)]$ fluorescence bands produced by OCS photoabsorption of extreme ultraviolet emission lines from λλ637-801 Å were analyzed and the cross sections for the production of fluorescence were measured. Several weak emission bands were identified as $A^2\Pi(000) \rightarrow X^2\Pi(v_1 00)$ transitions. No fluorescence emitted from the OCS^+ ion, other than from the $A^2\Pi(000)$ vibrational level, was detected.

I. Introduction

The total fluorescence produced by OCS photoabsorption of extreme ultraviolet radiation has been observed by Cook and Ogawa [1]. The fluorescence was later dispersed by Judge and Ogawa [2] and determined to be in part emitted from the $OCS^+[A^2\Pi(000)(i) \rightarrow X^2\Pi(00v)(i)]$ transitions. Here, the identification of weak bands in the emission spectrum has been extended through the use of higher resolution spectra and the cross sections for the production of fluorescence have been measured.

II. Experimental

The experimental setup has been described in a previous paper [3]. The nominal wavelength of the emission lines used in this investigation were λ637, 689, 704, 716, 769, 790, and 801 Å. The bandwidth of the 1-m normal incidence monochromator used to isolate these lines was set at 10 Å or less. The bandwidth of the 0.3-m monochromator used to disperse the fluorescence was set at 15 Å or less.

The absolute source line intensities were measured with a nickel film photoelectric detector, and the fluorescence was detected with a cooled photomultiplier (EMI 9659BM) which is equipped with a glass window so that it responds in the wavelength region λλ3000-9000 Å. The response of the combination of the 0.3-m monochromator and the photomultiplier for wavelengths longer than λ3100 Å is essentially the same as that published in a previous paper [4].

OCS gas supplied by the Matheson Gas Company with a purity greater than 97.5% was used without further purification. The pressure inside the sample cell as monitored with a Baratron Capacitance Manometer and was limited to a maximum of 15 mtorr, below which the fluorescence intensity was linear with gas pressure.

III. Results and Discussion

A. Fluorescence Spectrum

The fluorescence spectrum produced by OCS photoabsorption of primary photons of wavelength $\lambda 801$ Å is shown in Figure 1. This spectrum was obtained with a bandwidth of 15 Å and has the characteristics of all spectra produced by other primary photon wavelengths. The bandhead positions of the $OCS^+[A^2\Pi_\Omega(000) \rightarrow X^2\Pi_\Omega(00v)$; $\Omega=\frac{1}{2}$ and $\frac{3}{2}$, v=0-4] emission bands given by Horani et al.,[5] are used to identify the strong emission bands and are indicated in the Figure. The bandhead positions for the v = 5 and 6 bands are calculated by using the data [5] that the average decrement of the vibrational quantum energy for each vibrational quantum is 45 cm^{-1}.

The weak bands distributed among the strong bands, which have also been observed by Horani et al., [5] are possibly in part attributable to the $A^2\Pi_\Omega(000) \rightarrow X^2\Pi_\Omega(v_1 0 v_3)$ emission bands, where v_1, v_3 = 1,2,.... Using the ν_1 value [6] of 650 cm^{-1} for the $OCS^+(X^2\Pi)$ state, the wave numbers and wavelengths for the various bandheads of the $OCS^+[A^2\Pi_\Omega(000) \rightarrow X^2\Pi_\Omega(v_1 0 v_3)]$ transition are calculated and listed in Table I. As indicated in the Figure several of the weak bands occur at the calculated positions of the $A^2\Pi_\Omega(000) \rightarrow X^2\Pi_\Omega(v_1 0 v_3)$ transitions.

B. Band Strengths

When the bandwidth of the 0.3-m monochromator was set at 8 Å the Ω components of each strong band shown in Figure 1 were completely separated. Therefore, the radiation rates, $\dot{n}$, for the components of various emission bands could be obtained and averaged over several spectra, are listed in Table II. The radiation rate is measured by the area under the spectral envelope and corrected by the detection response. The band strength, which is defined [7] as $P=Re^2q = k\,\dot{n}\,\lambda^3$, is also

calculated and given in Table II, where Re is the electronic transition moment and q is the Franck-Condon factor. The radiation rate for the $\Omega = \frac{3}{2}$ component and the band strengths for both the $\Omega = \frac{1}{2}$ and $\frac{3}{2}$ components of the $A^2\Pi_\Omega(000) \rightarrow X^2\Pi_\Omega(003)$ band are normalized to 1. The Franck-Condon factors previously published by Judge and Ogawa [2] were only estimated from their low resolution spectra and are somewhat different from the present values.

C. Production Cross Sections

At low gas pressure, P., the radiation rate is given [4] by

$$\dot{n} = K \sigma_f \, Io \, P \, F(\lambda_f)$$

where K is a constant, σ_f is the fluorescence production cross section, and Io is the primary photon flux and $F(\lambda_f)$ is the wavelength dependent response function of the detection system.

The production cross sections for the sum of the $OCS^+[A^2\Pi_\Omega(000) \rightarrow X^2\Pi_\Omega(00v)$; $\Omega = \frac{1}{2}$ and $\frac{3}{2}$, v = 2-5] bands are obtained from the measured fluorescence radiation rates, and calibrated against the known fluorescence cross section of the N_2^+ first negative system [8]. The results for the production cross sections are listed in Table III for the various primary photon wavelengths. The thresholds for the production of OCS^+ [$A^2\Pi_\Omega(000)$, $\Omega = \frac{1}{2}$ and $\frac{3}{2}$] ions are at λ821.14 and 822.26 Å, respectively. The total absorption cross sections, σ_T, given by Cook and Ogawa [1] are adopted to calculate the production yields, $\eta(= \sigma_f/\sigma_T)$, which are also listed in Table III. The cross sections are in units of Mb ($= 10^{-18}$ cm^2) and the yields are in %.

IV. Concluding Remarks

The photoelectron spectrum [6] of OCS^+ shows three well defined states, $A^2\Pi$, $B^2\Sigma^+$, and $C^2\Sigma^+$, which are very similar to CO_2^+. However, in contrast to CO_2^+ which emits fluorescence [3] from all excited vibrational levels of the $A^2\Pi_u$ state and the ground level of the $B^2\Sigma_u^+$ state, OCS^+ emits no fluorescence from levels higher than v = 0 of the $A^2\Pi$ state. Judge and Ogawa [2] have attributed the absence of fluorescence from the $V \geq 1$ levels of the $A^2\Pi$ state to predissociation. This assertion is further strengthened by the present observation that the cross section for production of fluorescence from the inverted $A^2\Pi_{1/2}$ (000) level is only 75% of that in the $A^2\Pi_{3/2}$(000) level. The relative fluorescence cross sections are measured by the sum of $\dot{n}\lambda$ [3] over all the bands listed in Table II.

The absence of fluorescence from the OCS^+($B^2\Sigma^+$ and $C^2\Sigma^+$) states indicates that these states are also predissociated.

Table I

The wave numbers, $\nu(cm^{-1})$, and the wavelengths, $\lambda(\mathring{A})$, for the various band heads of the $A^2\Pi_\Omega(000) \rightarrow X^2\Pi_\Omega(v_1 0 v_3)$ transitions.

Ω	v_1		v_3 = 0	1	2	3	4	5	6
$\frac{1}{2}$	0	ν	31154*	29091*	27066*	25088*	23158*	21269	19425
		λ	3208.9*	3436.5*	3693.6*	3984.9*	4317.0*	4700.3	5146.5
	1	ν	30504	28441	26416	24438	22508	20619	18775
		λ	3277.3	3515.0	3784.5	4091.0	4041.6	4848.5	5324.7
	2	ν	29854	27791	25766	23788	21858	19969	18125
		λ	3348.7	3597.2	3880.0	4202.6	4573.7	5006.3	5519.5
$\frac{3}{2}$	0	ν	31408*	29339*	27316*	25334*	23400*	21511	19667
		λ	3183.0*	3407.4*	3659.8*	3946.2*	4272.2*	4647.2	5083.2
	1	ν	30758	28689	26666	24684	22750	20861	19017
		λ	3250.2	3484.7	3749.0	4050.0	4394.3	4792.0	5257.0
	2	ν	30108	28039	26016	24034	22100	20211	18367
		λ	3320.1	3565.5	3842.7	4159.6	4521.5	4946.0	5443.0

*Adopted from the data given by Horani et al.

Table II

The radiation rates, $\dot{n}$, and the band strengths, P, for the various bands of the $A^2\Pi_\Omega(000) \rightarrow X^2\Pi_\Omega(00v_3)$ emission system. The band positions, λ, are in units of Å.

Ω		v_3 = 2	3	4	5
$\frac{1}{2}$	λ(Å)	3693.6	3984.9	4317.0	4700
	$\dot{n}$	0.45	0.75	0.59	0.41
	P	0.48	1.00	0.99	0.89
$\frac{3}{2}$	λ(Å)	3659.8	3946.2	4272.2	4647.2
	$\dot{n}$	0.69	1.00	0.84	0.52
	P	0.55	1.00	1.07	0.82

Table III

Cross sections, σ(Mb), and the production yield, η(%), for fluorescence from the sum of the $OCS^+[A^2\Pi_\Omega(000) \rightarrow X^2\Pi_\Omega(00v_3)$; $\Omega = \frac{1}{2}$ and $\frac{3}{2}$, $v_3 = 2\text{-}5]$ bands. The total absorption cross sections, σ_T(Mb), for various primary photon wavelengths, λ(Å), are adopted from the data given by Cook and Ogawa.

λ(Å)	σ_f(Mb)	σ_T(Mb)	η(%)
637	0.05	41.8	0.12
689	0.06	45.8	0.13
704	0.05	45.5	0.11
716	0.05	45.0	0.11
769	0.06	46.1	0.13
790	0.06	42.4	0.14
801	0.11	71.5	0.15

Figure Caption

Fig. 1. Fluorescence spectra of the $OCS^+[A^2\Pi_\Omega(000) \rightarrow X^2\Pi_\Omega(v_1 0 v_3)]$ system produced by primary photons of wavelength λ801 Å. The bandhead positions given in Table I are indicated.

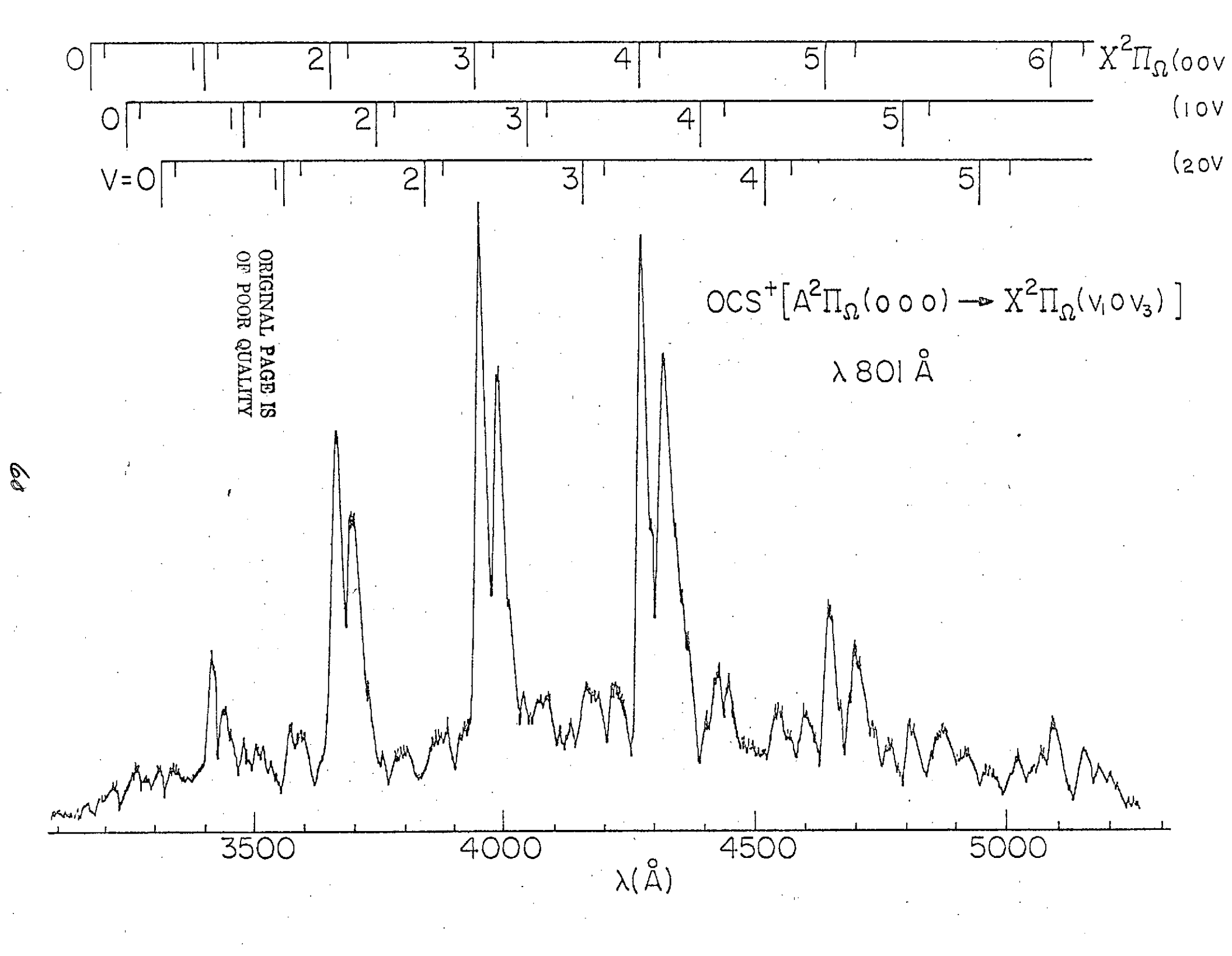
0 1 2 3 4 5 6 $X^2\Pi_\Omega$(00v
0 1 2 3 4 5 (10v
V=0 1 2 3 4 5 (20v
ORIGINAL PAGE IS
OF POOR QUALITY
$OCS^+[A^2\Pi_\Omega(0\,0\,0) \rightarrow X^2\Pi_\Omega(v_1\,0\,v_3)]$
λ 801 Å
3500
4000
4500
5000
λ(Å)

Acknowledgment

This work was supported by the National Aeronautics and Space Administration under Grant No. NGR 05-018-180.

REFERENCES

1 G. R. Cook and M. Ogawa, J. Chem. Phys., 51 (1969) 647.

2 D. L. Judge and M. Ogawa, J. Chem. Phys., 51 (1969) 2035.

3 D. L. Judge and L. C. Lee, J. Chem. Phys., 57 (1972) 455.

4 L. C. Lee and D. L. Judge, J. Chem. Phys., 57 (1972) 4443.

5 M. Horani, S. Leach, J. Rostas, and G. Berthier, J. Chem. Phys., 63 (1966) 1015.

6 C. R. Brundle and D. W. Turner, Int. J. Mass Spectrosc. Ion Phys., 2 (1969) 195.

7 R. W. Nicholls, J. Quant. Spectrosc. Radiat. Transfer, 2 (1962) 433.

8 D. L. Judge and G. L. Weissler, J. Chem. Phys., 48 (1968) 4590.

REEVALUATION OF THE $CO_2^+(X^2\Pi_g)$ BENDING QUANTUM

D. L. Judge and L. C. Lee
Department of Physics
University of Southern California
Los Angeles, California 90007

and

M. J. Haugh
Department of Chemistry
Temple University
Philadelphia, Pennsylvania 19122

The index classification of this paper is 5.442

ABSTRACT

With the assumption that the splitting of the $CO_2^+[X^2\Pi_g(100)(\frac{3}{2})]$ level is caused by perturbation of the $CO_2^+[X^2\Pi_g(020)(\frac{3}{2})\ G^+]$ level, the bending vibrational levels are calculated and the bending frequency, ω_2, is found to be 514.8 cm^{-1}. This value is comparable to the observed frequency of 513±10 cm^{-1} obtained from the $CO_2^+(A^2\Pi_u \rightarrow X^2\Pi_g)$ fluorescence spectra which are selectively produced by vacuum ultraviolet radiation.

I. Introduction

The bending quantum of the $CO_2^+(X^2\Pi_g(i))$ molecule has been previously measured by Judge et al. (1969). However, due to limited spectral resolution only an approximate value was given. Here its value has been remeasured using significantly higher resolution spectra.

The bending vibrational levels of $CO_2^+(X^2\Pi_g)$ are split by the spin-orbit and the vibronic interactions (Herzberg 1966). The lowest vibrational level splits into two sublevels and their terms are given by

$$G(0,1,\pm\tfrac{1}{2}) = \omega_2 \pm \tfrac{1}{2} A - \tfrac{1}{4}\varepsilon^2\omega_2 \qquad (1)$$

where $\pm\frac{1}{2}$ is the spin quantum number, ω_2 is the bending frequency, A is the spin-orbit interaction constant, and ε is the Renner parameter.

Each excited bending vibrational level is split into four sublevels and their terms are

$$G^+(v_2,1,\pm\tfrac{1}{2}) = \omega_2(1 - \tfrac{1}{8}\varepsilon^2)(v_2+1) + \tfrac{1}{2}A^*_{v_2,1} \mp \frac{\varepsilon^2 A\,\omega_2(v_2+1)}{8\,A^*_{v_2,1}} \qquad (2)$$

and, $$G^-(v_2,1,\pm\tfrac{1}{2}) = \omega_2(1 - \tfrac{1}{8}\varepsilon^2)(v_2+1) - \tfrac{1}{2}A^*_{v_2,1} \pm \frac{\varepsilon^2 A\,\omega_2(v_2+1)}{8\,A^*_{v_2,1}} \qquad (3)$$

where $A^*_{v_2,1} = \sqrt{A^2 + \varepsilon^2\omega_2^2\, v_2(v_2+2)}$

Mrozowski (1941, 1942, 1947a, and 1947b) has observed that the sublevel $\Omega = \frac{3}{2}$ of the $X^2\Pi_g(100)$ state is very strongly perturbed and splits into 1^a and 1^b sublevels. He suggested that the perturbation is probably caused by the $X^2\Pi_g(020)$ state. If we assume that the perturbing level is the $X^2\Pi_g(020)(\frac{3}{2})$ G^+ sublevel and its position is halfway between

the 1^a and 1^b levels, i.e., $G^+(2,1,+\frac{1}{2}) = 1264.6\ cm^{-1}$ measured from the $X^2\Pi_g(000)(3/2)$ level, then ω_2, calculated from equations (1) and (2) and the known values of $\epsilon\omega_2(= -93\ cm^{-1})$ and $A(= -159.5 cm^{-1})$(Herzberg 1966), is found to be $514.8\ cm^{-1}$. The Renner parameter is therefore $\epsilon = -0.18$. Using these ω_2 and ϵ values the positions of the bending vibrational levels are calculated as shown in Fig. 1.

II. Analysis

Fig. 2 shows the spectra obtained by photoionization of CO_2 at the primary photon wavelengths of λ715, 709, and 703 Å, of which the highest possible excited vibrational levels are $A^2\Pi_u(000)$, (100), and (200), respectively. The spectrum obtained by photon excitation at a wavelength of λ587 Å is shown in Fig. 3. The spectral bandwidth of the 0.3 m monochromator used to obtain these spectra was set at 4 Å or less.

As indicated in the spectra shown in Fig. 2 and 3, the emission bands of the $A^2\Pi_u(v_1 00)(\Omega) \rightarrow X^2\Pi_g(020)(\Omega)\ G^{\pm}$ transitions always accompany those of the $A^2\Pi_u(v_1 00)(\Omega) \rightarrow X^2\Pi_g(000)(\Omega)$ transitions. With the present spectra the wavelength for an emission band is determined within 3 Å (~30 cm^{-1}). However, checking with the previously published emission spectra (Smyth 1931; Fox et al., 1927) the positions of the emission bands are further confined and their wave numbers are determined within 10 cm^{-1}. The observed wave numbers for the various $A^2\Pi_u(v_1 00)(\Omega) \rightarrow X^2\Pi_g(020)(\Omega)\ G^{\pm}$ transitions are listed in Table 1. The calculated wave numbers, which are obtained from the known positions of the $A^2\Pi_u(v_1 00)$ levels (Mrozowski 1941, 1942, 1947a, 1947b) and the calculated energy levels shown in Fig. 1, are also listed in the table for comparison. The correctness of the assignment for the $A^2\Pi_u(v_1 00)(\Omega) \rightarrow X^2\Pi_g(020)(\Omega)\ G^-$ transitions is corroborated by

the fact that the vibrational energy of a $A^2\Pi_u(v_1 00)$ level obtained from its presently assigned transition to the $X^2\Pi_g(020)G^-$ level agrees with its transition to the $X^2\Pi_g(000)$ level assigned by Mrozowski (1941, 1942 and 1947a). The vibrational energies of the $A^2\Pi_u(v_1 00)$ levels obtained from their transitions to the different $X^2\Pi_g$ levels are listed in Table 2 for comparison.

The positions of the $X^2\Pi_g(020)(\frac{3}{2})$ and $(\frac{1}{2})$ G^- levels obtained from the observed emission bands listed in Table 1 and Table 2 are listed in Table 3. The average values for the positions of the $X^2\Pi_g(020)$ $(\frac{3}{2})$ and $(\frac{1}{2})$ G^- levels are 935 and 963 cm^{-1}, and in reasonable agreement with the calculated values 950.2 and 956.7 cm^{-1}, respectively.

From the spectrum produced by the primary photons of wavelength $\lambda 715$ Å the positions of the various $A^2\Pi_u(000)(\Omega) \rightarrow X^2\Pi_g(0v_2 0)(\Omega)$ $G^{\pm}$ emission bands are obtained and listed in Table 4. The position of the $A^2\Pi_u(000)(\frac{3}{2}) \rightarrow X^2\Pi_g(020)(\frac{3}{2})$ G^+ band is estimated from the 1^a and 1^b levels given by Mrozowski (1941 and 1942). The calculated positions of the expected emission bands are also listed in Table 4 for comparison. The positions of the bending vibrational levels obtained from these observed emission bands are comparable to the calculated levels and are shown in Fig.1, in which the positions of the $X^2\Pi_g(020)(\frac{3}{2})$ and $(\frac{1}{2})$ G^- levels are adopted from the average values listed in Table 3.

Since the quantity $\frac{1}{8}\varepsilon^2\omega_2$ is $\simeq 2$ cm^{-1} and within the experimental error, it may be neglected in the experimental determination of ω_2. The observed vibrational levels are plotted against the quantum number as shown in Fig. 4, in which the energy centroid of the sublevels is linear with quantum number. The observed bending frequency determined from such data is 513 ± 10 cm^{-1}.

Acknowledgment

The authors wish to thank professor Ogawa for his encouragement and comments on this analysis. This work was supported by the National Aeronautics and Space Administration under Grant No. NGR 05-018-180.

References

Fox, G.W., Duffendack, O.S., and Baker, E.F. 1927. Proc. Nat. Acad. 13, 302

Herzberg, G. (Editor), 1966. Electronic Spectra and Electronic Structure of Polyatomic Molecules (Van Nostrad Reinhold Co., N.Y.), pp. 36 and 594.

Judge, D.L., Bloom, G.S., and Morse, A.L. 1969 Can. J. Phys. 47, 489

Mrozowski, S. 1941 Phys. Rev. 61, 730

_____ 1942 Phys. Rev. 62, 270

_____ 1947a Phys. Rev. 72, 682

_____ 1947b Phys. Rev. 72, 691

Smyth, H.D. 1931 Phys. Rev. 38, 2000

. Table 1

Comparison between the calculated and the observed* wave numbers, ω_c and ω_o, for the $A^2\Pi_u(v_1 00)(\Omega) \rightarrow X^2\Pi_g(020)(\Omega)$ G^- transitions.

v_1 \ Ω	$\frac{1}{2}$			$\frac{3}{2}$		
	Wave Number (cm^{-1})			Wave Number (cm^{-1})		
	ω_c	ω_o	$\omega_c-\omega_o$	ω_c	ω_o	$\omega_c-\omega_o$
0	27671.3	27651	20	27582.3	27600	-18
1	28797.2	28802	-5	28709.1	28721	-12
2	29918.5	29911	8	29831.8	29844	-12
3	31034.1	31035	-1	30952	30972	-20

* Values are taken from Smyth (1931) and Fox et al. (1927)

Table 2

Comparison of the vibrational energies of the $A^2\Pi_u(v_1 00)(\Omega)$ levels obtained from their transitions to the $X^2\Pi_g(020)(\Omega)$ G^- level with their transitions to the $X^2\Pi_g(000)(\Omega)$ level.

V_1	Ω	$\omega_p^*(v_1)$ cm^{-1}	$\omega_o^*(v_1)$ cm^{-1}	Present $\omega_o(v_1) - \omega_o(0)$	Mrozowski $\omega(v_1)^{**} - \omega(0)$
0	$\frac{1}{2}$	27620±30	27651±10		
	$\frac{3}{2}$	27550	27600		
1	$\frac{1}{2}$	28790	28802	1151	1127
	$\frac{3}{2}$	28730	28721	1121	1126
2	$\frac{1}{2}$	29890	29911	2260	2250
	$\frac{3}{2}$	29820	29844	2244	2247
3	$\frac{1}{2}$	31050	31035	3384	3370
	$\frac{3}{2}$	30960	30972	3372	3372

* $\omega_p(v_1)$ and $\omega_o(v_1)$ are the wave numbers for the $A^2\Pi_u(v_1 00)(\Omega) \rightarrow X^2\Pi_g(020)(\Omega)$ G^- transition obtained from the present and Smyth's Spectra, respectively.

** $\omega(v_1)$ is the wave number for the $A^2\Pi_u(v_1 00)(\Omega) \rightarrow X^2\Pi_g(000)(\Omega)$ transition adopted from Mrozowski.

Table 3

The observed $X^2\Pi_g(020)(\Omega)$ G^- energy levels relative to the $X^2\Pi_g(000)(3/2)$ level. These levels are obtained from the observed wave numbers of the $A^2\Pi_u(v_1 00)(\Omega) \rightarrow X^2\Pi_g(020)(\Omega)$ G^- transitions listed in Table 1.

v_1 \ Ω	$\frac{1}{2}$	$\frac{3}{2}$
0	977±10 cm^{-1}	932±10 cm^{-1}
1	952	938
2	965	938
3	956	930
Aver-age	963	935

Table 4

Comparison between the calculated and the observed* wave numbers ω_c and ω_o, for the $A^2\Pi_u(000)(\Omega) \leftarrow X^2\Pi_g(0v_20)(\Omega)$ $G^{\pm}$ transitions.

v_1	Ω	$\frac{1}{2}$			$\frac{3}{2}$		
		Wave Number (cm^{-1})			Wave Number (cm^{-1})		
		ω_c	ω_o	$\omega_c-\omega_o$	ω_c	ω_o	$\omega_c-\omega_o$
2	G^+	27370.2	27390	-20	27268.2	27268.2	0
	G^-	27671.3	27651	20	27582.3	27600	-18
4	G^+	26257.5	26241	17	26155.0	26152	3
	G^-	26733.2	26718	15	26644.7	26561	-16

*Values are taken from Smyth (1931) and Fox et al. (1927)

FIGURE CAPTIONS

Fig. 1. The calculated and observed vibrational energies of the $CO_2^+[X^2\Pi_g(0v_20)(\Omega)]$ levels. The vibrational energies are relative to the $X^2\Pi_g(000)(\frac{3}{2})$ level and in units of cm^{-1}.

Fig. 2. The fluorescence spectra of the $CO_2^+(A^2\Pi_u \rightarrow X^2\Pi_g)$ system produced by primary photon wavelengths λ715, 709, and 703 Å. The positions of the $A^2\Pi_u(v_1'00) \rightarrow X^2\Pi_g(v_1''00)$ and $X^2\Pi_g(0v_2''0)$ G transitions are indicated.

Fig. 3. The fluorescence spectrum of the $CO_2^+(A^2\Pi_u \rightarrow X^2\Pi_g)$ system produced by primary photon wavelengths λ587 Å. The positions of the $A^2\Pi_u(300) \rightarrow X^2\Pi_g(v_1''00)$ and $X^2\Pi_g(020)$ transitions are indicated.

Fig. 4. The plot of the observed vibrational energies, $\omega(cm^{-1})$, versus the vibrational bending quanta, v_2, for the $X^2\Pi_g(0v_20)$ levels. A line through the energy centroid is drawn.

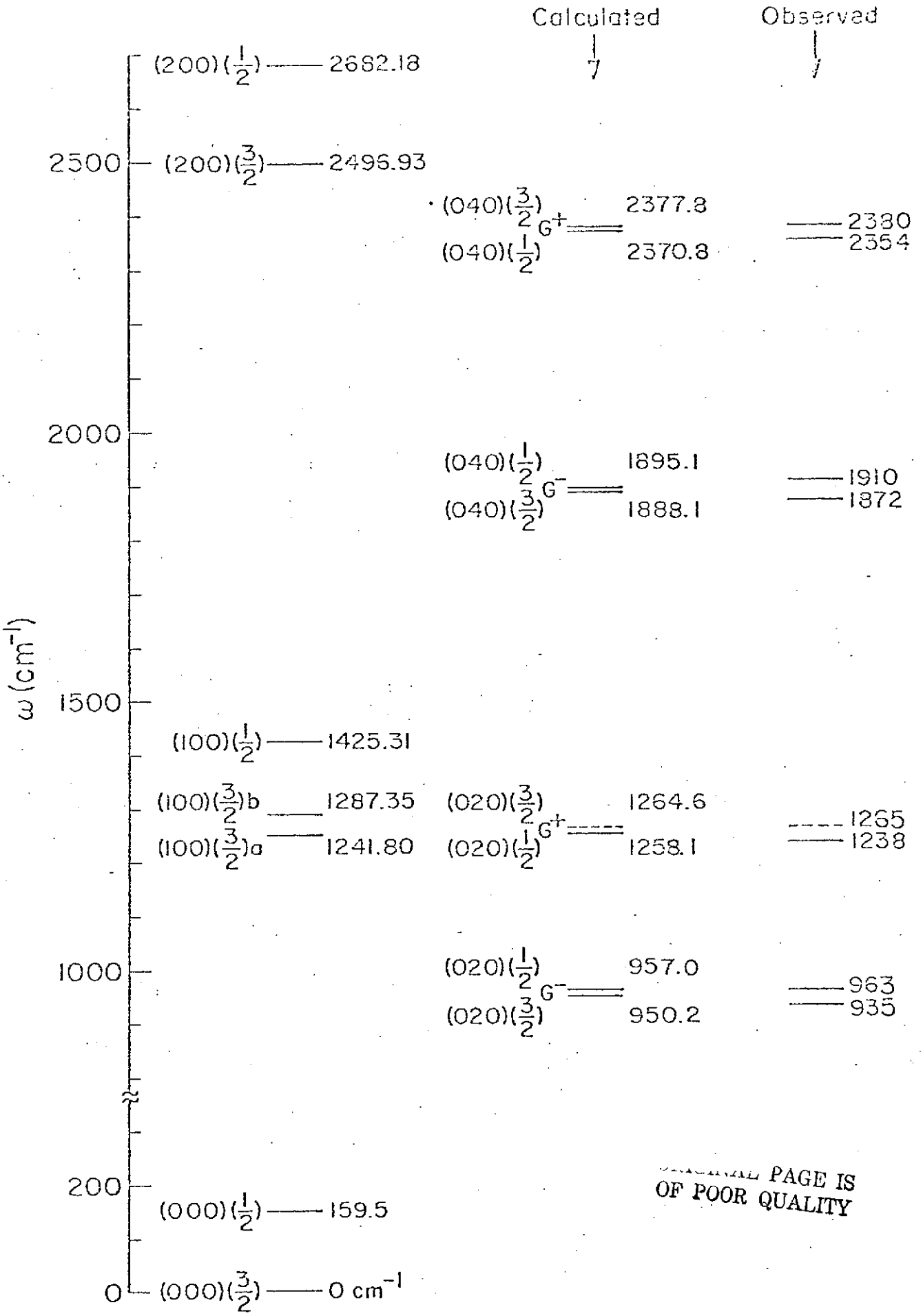

Figure 1

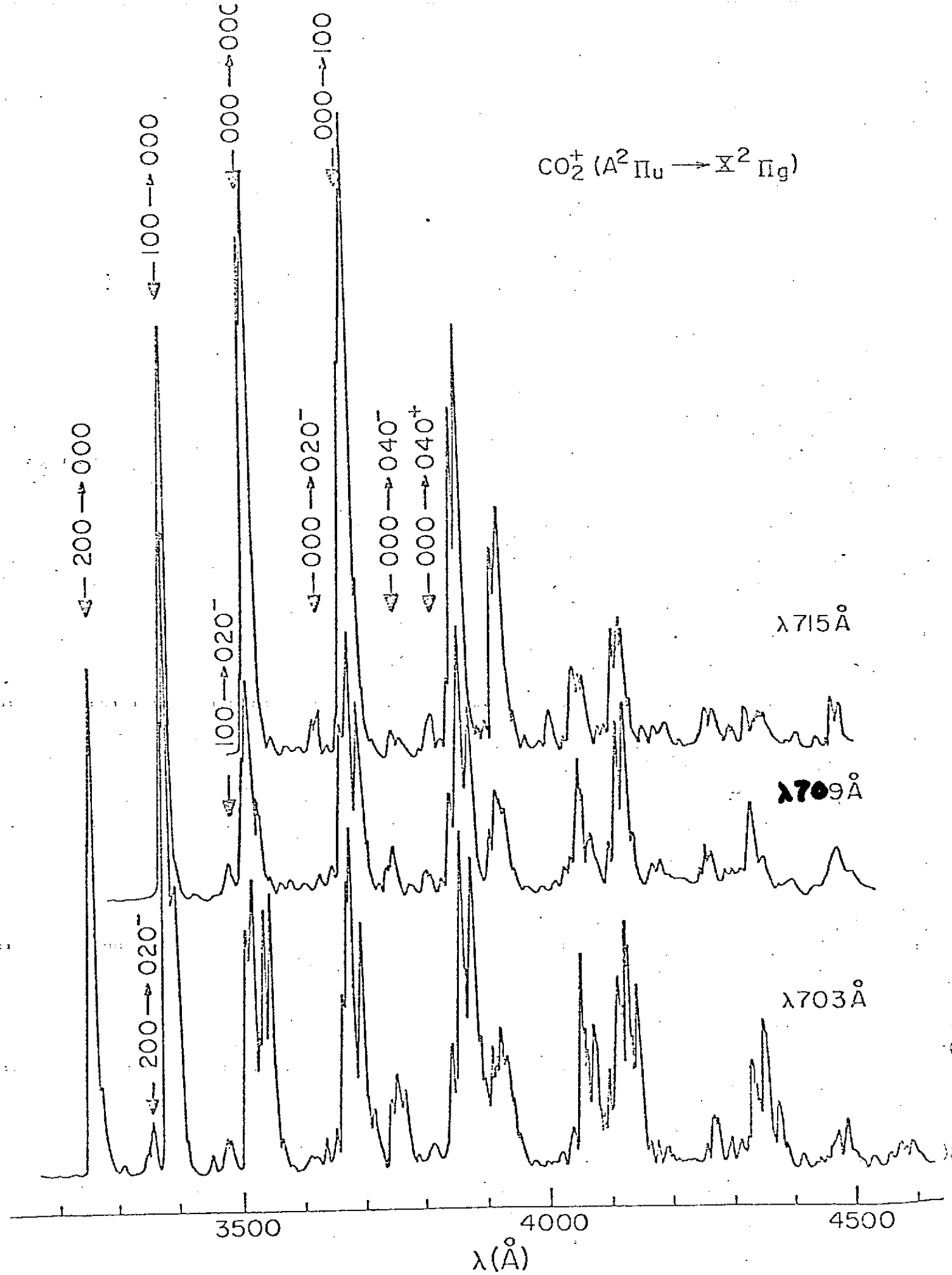
$CO_2^+ (A^2\Pi_u \rightarrow X^2\Pi_g)$
200 → 000
100 → 000
000 → 000
000 → 100
100 → 020⁻
000 → 020⁻
000 → 040⁻
000 → 040⁺
200 → 020⁻
λ715Å
λ709Å
λ703Å
3500
4000
4500
λ(Å)

Figure 2

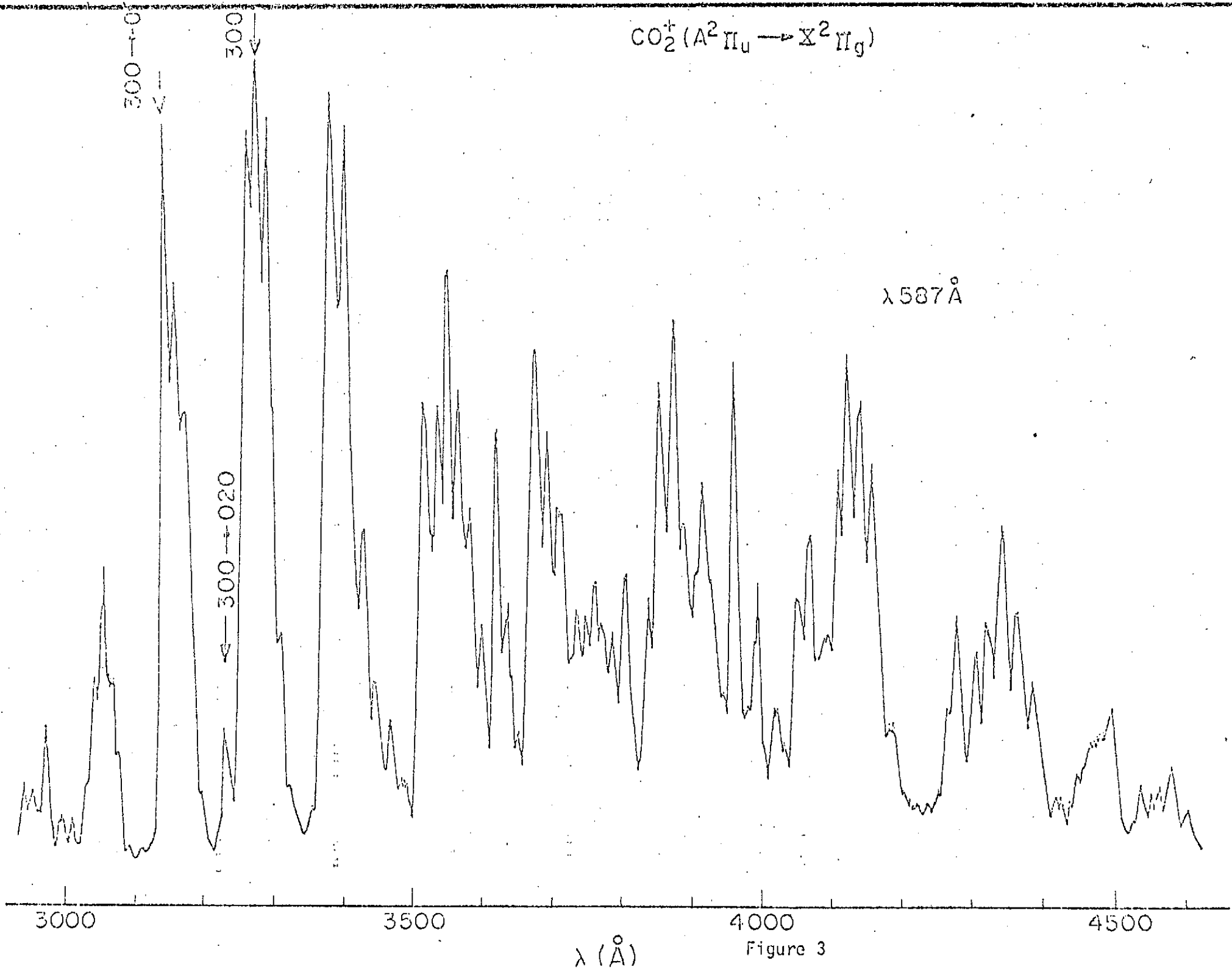
$CO_2^+(A^2\Pi_u \rightarrow X^2\Pi_g)$
λ587Å
300←0
300
300←020
3000
3500
4000
4500
λ (Å)

Figure 3

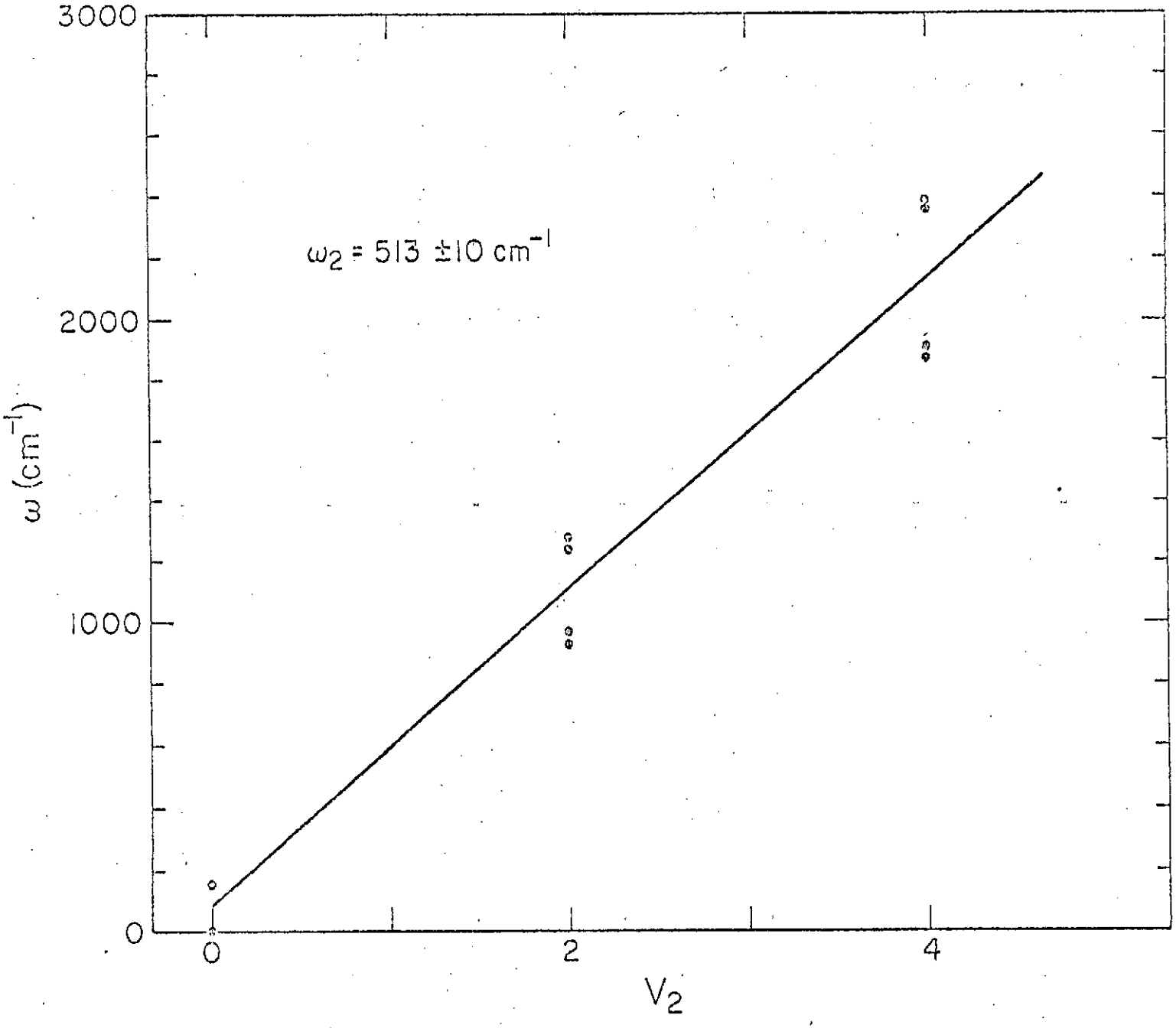

Figure 4

APPENDIX A

CONTINUATION PROPOSAL (April 26, 1972)

INTRODUCTION

The following proposal indicates the areas of work successfully pursued during the past funding period and suggests a logical extension of the past effort. Our work is concerned with the measurement of absolute photodissociation cross sections for the formation of specific products of the atmospheric gases and long term evaluation of channeltrons.

PHOTON IMPACT STUDIES OF MOLECULAR GASES

I. Measurements of the Absolute Cross Sections

The cross sections for the production of molecular fragments by XUV irradiation have been measured by observing the fluorescence radiation rates from those fragments. The experimental arrangement is shown in Fig. 1. The XUV light was produced by a spark discharge through a boron nitride capillary and dispersed with a 1-m normal incidence monochromator (McPherson 225). The fluorescence produced by the molecular fragments was dispersed with a 0.3-m normal incidence monochromator (McPherson 218) and detected synchronously with a cooled EMI 9558 QB photomultiplier. The absolute cross sections were determined by comparing the fluorescence radiation rates of the molecular fragments with that of $N_2^+(B\ ^2\Sigma_u^+)$. The absolute cross sections for the production of some excited fragments from CH_4, and CO_2 have been measured in this laboratory (see Appendix A and B). Using the same facilities and techniques, the absolute cross sections for the gases of interest in planetary atmospheres, such as NH_3, H_2O, NO, N_2O, NO_2, etc. will be measured during the next funding period.

II. The Population Distribution of Excited Vibrational Levels Produced by Photodissociation

The mechanism for the production of the CO Cameron bands through photodissociation of CO_2 has been studied in this laboratory during the past year. It is found that the dominant mechanism is as given below:

$$CO_2 + h\nu \rightarrow CO_2^*$$

$$\rightarrow CO(a'^3\Sigma^+,\ d\ ^3\Delta_i,\ e\ ^3\Sigma^-) + O(^3p)$$

$$\rightarrow CO(a\ ^3\Pi) + O(^3p) + h\nu'$$

The population distribution of the vibrational levels of $CO(a'^3\Sigma^+$ and $d\ ^3\Delta_i)$ has been found to be a Poisson distribution and agrees with the prediction of a quasidiatomic model, which is characterized only by the phase-average transfer energy during the separation period (see Appendix C). This model should, however, be tested in the photodissociation of other gases of atmospheric interest. In particular, it would be highly desirable to test the validity of the model by observing the photodissociation of other linear molecules, such as N_2O, NO_2 and CS_2. The fluorescence from the fragments of these molecules has been previously observed in photodissociation. The fragments formed are,

$$N_2O + h\nu \rightarrow N_2^* + O \rightarrow N_2 + O + h\nu'$$

$$NO_2 + h\nu \rightarrow NO^* + O \rightarrow NO + O + h\nu'$$

and

$$CS_2 + h\nu \rightarrow CS^* + S \rightarrow CS + S + h\nu'$$

The population distribution of the vibrational levels of these fragments can be measured by the same technique as used to study CO_2.

III. Constancy of the Transition Dipole Moments vs. Internuclear Distances for Molecular Transitions

The electronic transition dipole moment of a molecular transition can be calculated using the measured radiation rates and the relative Franck-Condon factors. Its variation with internuclear distance has been studied by several authors, but substantial errors are present in the many of the published papers. Using the line emission light source and the synchronous detection system, it is possible to produce accurate data, and accordingly to determine the transition dipole moments with

precision. The transition dipole moments of the A→X, B→X, and B→A systems of CO^+ have been investigated. In contrast to a previous result indicating that the transition dipole moment of the A→X system of CO^+ varies with the internuclear separation it is found that each system has a constant transition dipole moment (see Appendix D). Since the transition dipole moment is a principal factor in the determination of the band strength, its measurement is important for the investigation of airglow measurements in planetary atmospheres. The measurement of transition dipole moments will be extended to several transitions of N_2, NO, and CS, during the next funding period.

IV. Quenching

In the study of the pressure dependence of the fluorescence intensity, it is, in general, observed that the fluorescence intensities for the lower vibrational levels decrease slower than the higher levels as the pressure increases. This relative intensity enhancement for the lower vibrational levels is attributed to the vibrational relaxation of the higher levels into the lower ones. The vibrational relaxation time may be obtained from a quantitative study of the pressure dependence of the fluorescence intensity. On the other hand, the measurement of the vibrational relaxation times will aide in the determination of the pressure of the gases in planetary atmospheres. Further study of this subject is planned.

V. Resonance Scattering Experiments

Consider the problem of determining the absolute cross section for the following photon-molecule interaction;

$$CO_2(\tilde{X}\ ^1\Sigma_g^+) + h\nu \rightarrow CO(a\ ^3\Pi) + O(^3p)$$

Assuming the incident photon flux is known, cross sections can be experimentally determined if the abundance of $O(^3p)$ is known. The amount of $O(^3p)$ present can be determined through the technique of resonance scattering.

Previously, cross sections in this laboratory have been determined through fluorescence studies of excited fragments. For the above reaction this would be a poor method since the fluorescence results from the "forbidden" transition [$CO(a\ ^3\Pi) \rightarrow CO(X\ ^1\Sigma^+)$]. Thus many of the $CO(a\ ^3\Pi)$ states would be depopulated through collisions. To determine this loss, deactivation rates are required. This makes the experiment difficult to perform and increases the possibility of error. Lawrence[1] has, however, observed this fluorescence and obtained a value for the deactivation coefficient and for the cross section for the production of $CO(a\ ^3\Pi)$. Nonetheless, an independent measurement not subject to the same experimental difficulties would be highly desirable.

Furthermore, there are many reactions which only yield fragments in their ground state. Resonance scattering could be used to assign cross sections to these processes. The reverse experiment can also be performed; if the reaction cross section is known and the resonance scattering cross section unknown, then it can be found experimentally.

Realizing the abundance of information that can be gathered through such scattering experiments this laboratory has intiated a study of resonance scattering. The following describes this work.

A. Work in Progress

Succesful observation of resonance scattering in helium have been made in this laboratory. Using the 584Å line of He I, resonance scattering

has been observed at right angles to the incident 584Å radiation when helium was introduced into the sample cell. An rf discharge through helium was used to generate the 584Å line. The self-absorption of this line by the source itself, has been studied using a 3-meter spectrograph in 4th order. It was found that the center of the line showed total absorption having a 0.01Å width at 100μ pressure through a path length of 4 cm. The self-absorption by the source is expected to be much less for diatomic gases such as O_2. Since the dominant background gas will be O_2, rather than O from which the 1304 radiation is obtained. The direction of gas flow through the discharge tube can also be used to further reduce the absorption.

At the present time an experiment is being assembled to study reactions through resonance scattering. The first reaction to be studied is $CO_2 + h\nu \rightarrow CO(a\ ^3\Pi) + O(^3p)$. What follows is a description of the experiment and an outline of the equipment available.

A photomultiplier, 1/2-meter Seya-Namioka type monochromator, and a 0.3-meter McPherson 218 monochromator are all attached to a sample cell. The optic axes of the components are connected in such a manner as to be mutually orthogonal. Also attached to the cell and on the optic axis of the McPherson monochromator is a Wood's horn light trap. A schematic diagram of the apparatus is shown in Fig. 2.

The McPherson monochromator is used to isolate the 1302Å resonance line of OI generated in an rf discharge tube containing O_2. After passing through the cell this radiation is trapped by the light trap. Thus the only 1302Å radiation which can reach the detector must be resonantly scattered. The present detector will use sodium salicylate in conjunction with a photomultiplier with a

blue sensitive photocathode. For the future a photomultiplier with a potassium bromide photocathode is proposed.to cover the wavelength range from 1050-1600Å.

The CO_2 will be dissociated primarily by radiation exiting from the 1/2-meter Seya-Namioka type monochromator. This monochromator is being built at USC and is just nearing completion. It employs differential pumping slits, sine bar drive, fast pumping, 1/2 meter Rowland circle for increased light gathering power and a stainless steel vacuum chamber.

A condensed spark discharge light source will be mounted at the monochromator entrance slit. Since this source generates a line emission spectrum resolution is generally not sacrificed by using the 1/2-meter monochromator.

Platinum and sodium salicylate coated photomultiplier detectors will be used to monitor the resonance line intensity and the incident photon intensity. These detectors will be calibrated using an argon ionization cell.

The output from the resonance scattering detector will be processed by gated pulse counting electronics synchronized with the spark source in order to increase the signal to noise ratio.

B. Summary

It is proposed that the technique of resonance scattering be established as a useful method for detecting ground state fragments. To this end it is suggested that a study be made of the reaction $CO_2 + h\nu \rightarrow CO(a\ ^3\Pi) + O(^3P)$, through resonance scattering from the $O(^3P)$, to yield an absolute cross section for the formation of CO in the a $^3\Pi$ state.

Ideally the only radiation reaching the detector would be 1302Å resonant scattered radiation. However since the sodium salicylate coated photomultiplier has a wide spectral response it will be necessary to make a difference measurement between the signal output when the resonant light source is turned on and when it is off. Thus non-resonant radiation, namely fluorescence, can be discriminated against. This method is applicable if radiation does not result from fluorescence excited by the resonance line.

Any "contaminating" fluorescence will result primarily from the Cameron bands, $CO(a\ ^3\Pi \rightarrow X\ ^1\Sigma^+)$, and excited CO_2^*. Other energetically possible processes are $CO_2 + h\nu \rightarrow CO(X\ ^1\Sigma^+) + O(^1D)$ and $CO_2 + h\nu \rightarrow CO(X\ ^1\Sigma^+) + O(^1S)$, but it is extremely difficult to detect any radiation from these long lifetime metastable states.

For those cases where competing fluorescence is a great problem a third monochromator could be used to isolate the scattered radiation. An alternate choice, which is less effective but also less expensive, is to use a narrow spectral response detector, such as the proposed potassium bromide photocathode photomultiplier.

[1] G. M. Lawrence, to be published in J. Chem. Phys. April 1972.

CHANNELTRON EVALUATION

I. Bendix 4028 Lifetime Studies

The evaluation of Bendix 4028 Channeltron multipliers is continuing with primary emphasis on determining their lifetime. Five of these devices are presently being tested and have accumulated $\approx 3 \times 10^{11}$ counts. They are now accumulating counts at the rate of $\approx$ 36,000 counts/sec. Periodically their gain and pulse height distribution is checked. To date no significant change in their characteristics has been observed after the initial "burn in" of $\approx 10^{9}$ counts. A sixth multiplier having an accumulated counts of 6×10^{11} counts is being transferred to the ion-pumped chamber containing the above referenced multipliers. Details of the channeltron characteristics will be included in the next progress report.

It is proposed that the lifetime evaluation be continued during the next funding period in order to provide further data on their expected behavior during multiyear missions such as those planned for the outer planets.

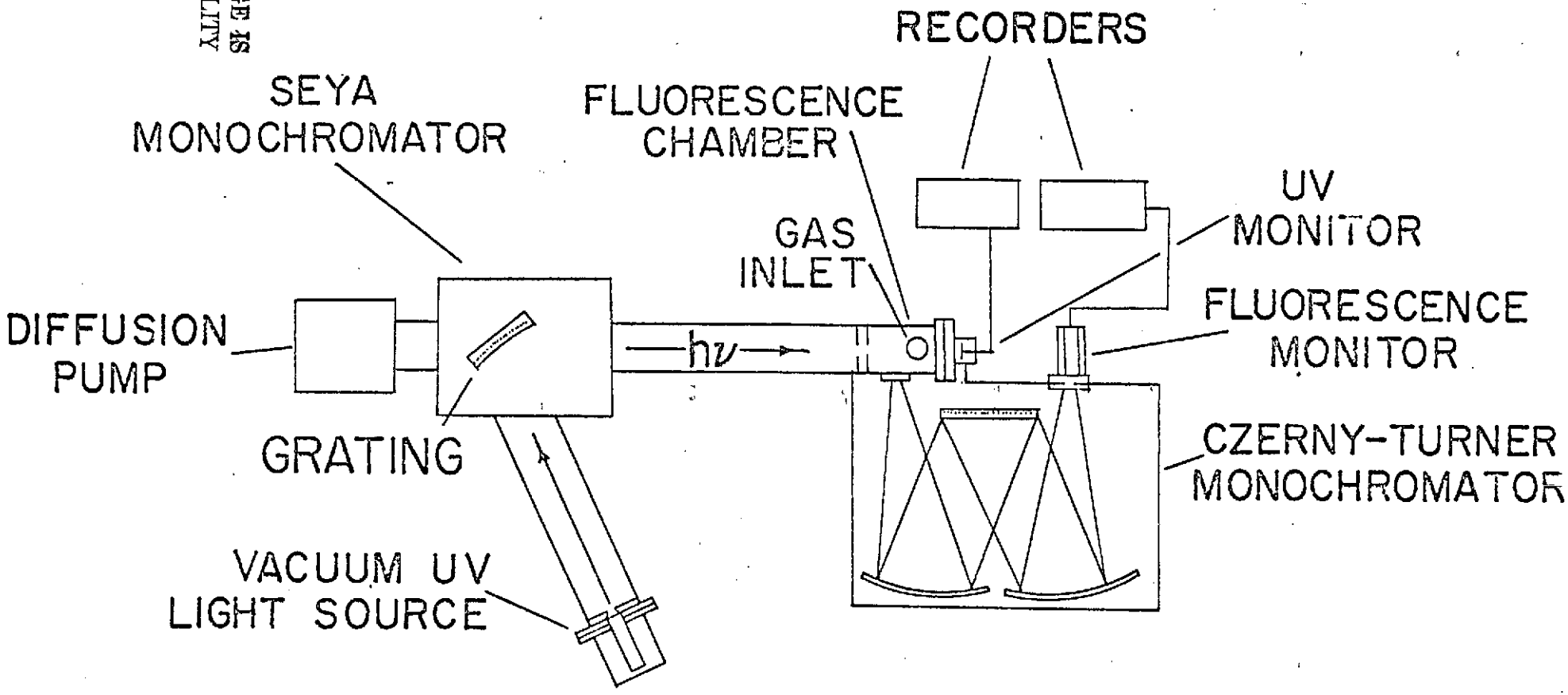

FIG. I. EXPERIMENTAL APPARATUS

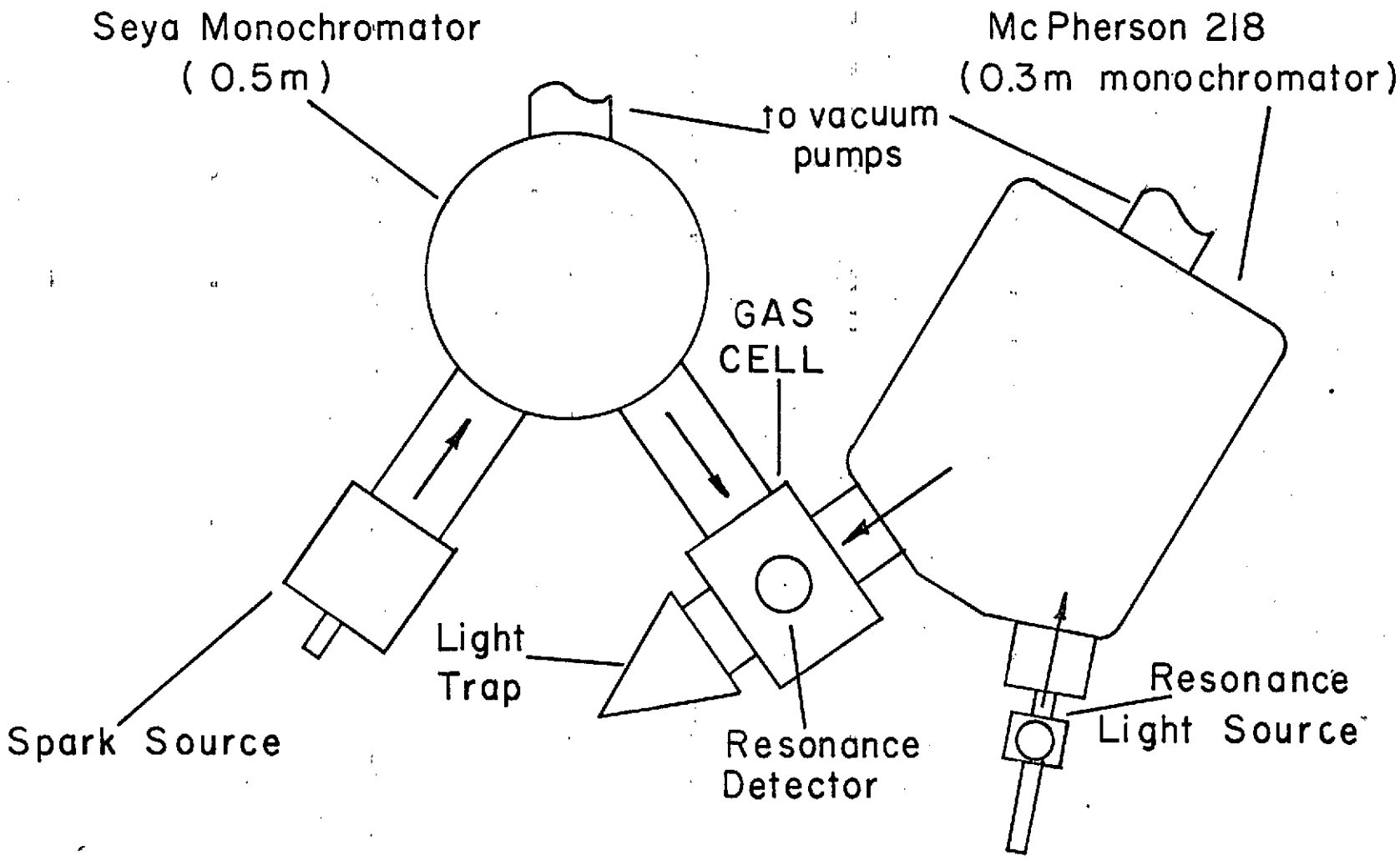

Fig. 2. Resonance Scattering Experimental Arrangement.

APPENDIX B

CONTINUATION PROPOSAL (July 10, 1973)

Abstract

The research proposed in the following sections represents a continuation of our laboratory investigations of processes of interest in planetary atmospheres. Primary emphasis will be placed on photodissociation processes leading to ground state or metastable fragments as outlined in Section I. Continuation of our evaluation of the long term characteristics of channeltrons is also proposed.

PHOTON-MOLECULE INTERACTION STUDIES OF THE ATMOSPHERIC GASES

I. DISSOCIATION CROSS SECTION MEASUREMENTS

INTRODUCTION

It is proposed to extend our preliminary investigation of gaseous photodissociation and photoionization processes which result in the formation of ground state and metastable atoms and molecules. Previous work in this laboratory has been involved primarily with the production of excited states in photon-molecule interactions. Such excitation processes were investigated by observation of the resulting fluorescence radiation. In the proposed extension these fluorescence emissions will be absent or weak owing to the long lifetime and deactivation of the metastable states. In this case detection of the ground state and metastable photo-fragments will be accomplished through resonance scattering. In addition to our own initial efforts such techniques have been used in the laboratory, for example, by Slanger and Black (1970) to detect ground state atomic oxygen and by Melton and Klemperer (1972) for NO detection. In the following paragraphs we discuss some of the specific processes to be investigated, considering O_2 as an example, followed by a brief discussion of the experimental aspects.

DISSOCIATION OF MOLECULAR OXYGEN

The absorption spectrum of oxygen exhibits the well known Schumann continuum in the 1400-1800Å region. This absorption is thought ot occur via excitation to the continuum of the $B^3\Sigma_u^-$ state followed by dissociation to produce $O(^3P) + O(^1D)$. Fluorescence of the $O(^1D)$ atoms produces the 6300Å multiplet. This feature is a strong component in the airglow spectrum and is attributed, in part, to photodissociative excitation by the solar ultraviolet. In recent years, however, concern has been

expressed that other states which could produce two $O(^3P)$ atoms rather than the $O(^3P) + O(^1D)$ products may be involved in the Schumann continuum. If such processes do occur, the quantum yield of $O(^1D)$ could be significantly different than previous assumptions would give. Laboratory information concerning the relative yields of $O(^3P)$ and $O^1D)$ are necessary for comparison with airglow measurements and the importance of photodissociation relative to other excitation mechanisms.

A somewhat similar situation is found for the OI λ5577Å line arising from $O(^1S)$. Recent airglow measurements (for example, Schaeffer et al., 1972) have suggested that a photodissociative excitation mechanism is important for $O(^1S)$ in addition to $O(^1D)$. This mechanism was discussed almost twenty years ago by Bates and Dalgarno (1954) who found that a lack of basic laboratory data prevents any reliable estimate of the contribution to the green airglow line due to photodissociation. This situation continues to be true, although the photodissociative excitation of $O(^1S)$ has been verified in observing 5577Å fluorescence produced by the ultraviolet flash photolysis of O_2 (Filseth and Welge, 1969). Tanaka (1952) has examined the absorption spectrum of O_2 and found minor peaks, one of which at 1293Å he suggests results in the formation of $O(^1S)$. At present, however, the cross section and states involved must be considered unknown.

At shorter wavelengths, oxygen still undergoes photodissociation. The total photodissociation cross section below ~ 1000Å has been obtained by Matsunaga and Watanabe (1967) and Cook et al. (1972). Certain of these continua have been identified but a complete description of the underlying processes has not yet been determined.

62

At shorter wavelengths the process of dissociative ionization can produce atoms (and atomic ions) in ground or excited states. Recent measurements indicate a rather high efficiency for this process not only for oxygen but other molecules also. Detection of the resulting photofragments and determination of the cross sections may be accomplished by resonance scattering.

EXPERIMENTAL ASPECTS

Measurements of the production of ground state and metastable atoms can be obtained through resonance scattering with the following basic experimental elements: a pulsed ultraviolet source to photodissociate the molecules in the experimental chamber, a source of resonance line photons, and a detector of the resonantly scattered radiation. Proper interpretation of the detected scattered radiation requires that several precautions be taken. First, if one is detecting ground state atoms (for example) one should insure that these atoms are created in the photodissociation process and not through secondary reactions. Some of these secondary processes of concern are the deactivation of metastable atoms produced in photodissociation, ground state atoms resulting from the radiative decay of excited photodissociation products, and atomic fragments arising from dissociative recombination and photoelectron excitation.

In order to estimate the relative contributions of these processes it is useful to envision a typical experiment. With sample gas partial pressures of 10 - 100 μ the absorption coefficient of the dissociating ultraviolet will be approximately 10^{-2} to 10^{-1} cm^{-1}. The mean free path at these total pressures is $\sim$ 0.05 to 0.5 cm with collision times of $\sim$

1 - 10 μ sec. Thus, the time to diffuse 1 cm is ~ 40 μ sec at 10 μ total pressure and 400 μ sec at 100 μ. If a buffer gas, for example a rare gas, is added, the diffusion time will vary approximately as the pressure. A 1 torr buffer gas will then increase the diffusion time to a few msec.

The light sources employed frequently in this laboratory are condensed spark discharges operated at pulse rates of ~ 50 Hz, each pulse lasting for times of a few μ sec. Typical line fluxes measured at the exit slit are ~ 2×10^8 photons/pulse, corresponding to an instantaneous rate of ~ 10^{14} photons/sec. Thus, with 1 percent absorption per cm each pulse produces ~ 10^{12} absorptions cm^{-1} sec^{-1}. While several other sources might be used for such work, data quality and subsequent interpretation are significantly enhanced by using a pulsed source having high instantaneous flux levels. . .

We can now estimate the order of magnitude contributions of the secondary processes. For dissociative recombination, each pulse will contribute $kn_+n_-\tau$ recombinations where k is the recombination coefficient, n_+, n_- are the ion and electron densities and τ is the diffusion time. The electrons will, of course, diffuse much faster than the ions, but we use here the ion diffusion time as a generous upper limit. In doing so, we find the rate of dissociative recombination is of order 1 - 10 per pulse and is much less than expected photodissociative processes. If one is working at wavelengths greater than the ionization potential, there will be no dissociative recombination contribution.

The photoelectron excitation rate can be estimated by assuming a cross section of 10^{-17} cm^2, a reasonably optimistic value considering

the low photoelectron energies that will be encountered. The probability of excitation is then approximately 3% of the primary absorption rate. If the photodissociation cross section is only a small fraction of the total absorption cross section, and if the electron dissociation cross section is as large as estimated, then this secondary process may be of concern. Pressure dependence measurements will be of value in experimentally evaluating the effect. Of course, at the longer wavelengths, there will be an absence of photoelectrons with sufficient energy for subsequent dissociative reactions and the effect can be neglected.

The production of ground state and metastable atoms from the radiative decay of excited photodissociation products will occur at the radiative transition rate, typically a few n-sec, and will be proportional to the photodissociative excitation rate. Since this time is much shorter than the primary light source pulses, no experimental discrimination of these products can be employed. Fortunately, these cross sections can be measured by observation of the resulting fluorescence giving a means of determining the cross section for the direct production of ground and metastable state atoms.

Deactivating collisions will destroy the metastable atoms and increase the concentration of ground state atoms over that produced directly in the photodissociation process. Consequently, measurement of either metastable or ground state atoms by resonance scattering must take this process into account for proper interpretation of the results. The time scale for this process can be estimated using measured deactivation coefficients. For the $O(^1D)$ state deactivated by O_2, $k \cong 5 \times 10^{-11}$ cm^3/sec

and at 100 μ partial pressure of O_2, $\tau \sim 7$ μ sec. For $O(^1S)$ the rate is approximately two orders of magnitude less, giving a mean life for $O(^1S)$ atoms of ~ 1 msec. Working at lower O_2 partial pressures will increase the lifetime against deactivation in proportion (if the buffer gas doesn't also participate), at the same time decreasing the primary rate of excitation.

These considerations suggest the experimental arrangement to be employed in further experiments. A pulsed spark source and vacuum spectrometer will be used to provide the initial photodissociation. Synchronously with this primary excitation, a condensed discharge lamp will be fired which will provide the necessary resonance line, e.g. λ 1302, 4, 6 Å radiation for detection of $O(^3P)$, λ 1152 Å for $O(^1D)$, and λ 1217 Å for $O(^1S)$. The sample time of the scattered resonance line should be a few μ sec for $O(^1D)$, $O^3P)$ and can be greater for $O(^1S)$. The deactivation coefficient and the relative contribution of these processes can be studied by varying the time delay between the primary light flash and the resonance scattering emission sampling time. In these experiments the resonance emission light source should directly illuminate the absorption cell and a solar blind photomultiplier directly view the resonantly scattered radiation. Either filters or a high throughput monochromator can be used to isolate the emission of interest.

II. CROSS SECTIONS FOR THE PRODUCTION OF FLUORESCENCE

Cross sections for production of fluorescence from $CO^+(A^2\Pi_i, B^2\Sigma^+ \rightarrow X^2\Sigma^+)$, $CO_2^+(A^2\Pi_u, B^2\Sigma_u^+ X^2\Pi g)$, and $N_2O^+(A^2\Sigma^+ \rightarrow X^2\Pi)$ (see appendices A, B, C) and from fragments of CH_4 and CO_2 (see appendices D and E) have been observed in the wavelength region from 462-1250Å. Using similar techniques the fluorescence production cross sections for these gases and others of interest in planetary atmospheres (O_2, N_2, NO, COS, H_2O, H_2S etc.) will be measured during the next funding period. Particular consideration will be given to resolving an existing problem concerning the production of the $CO_2^+(A, B \rightarrow X)$ fluorescence. Photoelectron spectroscopy results give, at 584Å, a production cross section for A/B = 0.65 while the fluorescence data imply A/B = 2.7. At present there is no satisfactory theoretical explanation for such a result. A possible source of the discrepancy is a systematic error introduced by the experimental arrangement. It is accordingly desirable to repeat the photoelectron data at 584Å using a 4π geometry in order to be sure that all photoelectrons are properly analyzed.

In addition to the work cited in the appendices, the fluorescence from the fragments of N_2 and NO by photodissociation of N_2O have been observed in this laboratory. However, an improvement of the present detection system is required to enhance the signal to noise ratio.

The relative fluorescence cross sections for the fragments of N, O and CO by photodissociation of N_2, O_2 and CO_2 have been observed using synchrotron radiation of 175-800Å (for example, see appendix F). Absolute measurement of the fluorescence cross sections using a strong line emission source in this laboratory will permit an absolute calibration of these relative measurements. It is accordingly proposed that the absolute cross section measurements be continued.

III. MEASUREMENTS OF THE POPULATION DISTRIBUTION OF EXCITED VIBRATIONAL LEVELS PRODUCED BY PHOTODISSOCIATION

The population distribution of triplet vibrational levels of CO produced by photodissociation of CO_2 has been measured in the previous funding period (see appendix G). The population is reasonably represented by a Poisson distribution and an internal collision mechanism was suggested to interpret the photodissociation process. For further study of this mechanism the vibrational populations of the CO, N_2, NO and CS fragments produced by the following photodissociation processes will be measured:

$$CO_2 + h\nu \rightarrow CO\ (A^1\Pi) + O$$

$$N_2O + h\nu \rightarrow N_2\ (B^2\Pi_g,\ C^3\Pi_u) + O$$

$$N_2O + h\nu \rightarrow NO\ (A^2\Sigma^+,\ B^2\Pi) + N$$

$$COS + h\nu \rightarrow CO\ (A^1\Pi,\ \text{triplet}) + S$$

$$COS + h\nu \rightarrow CS\ (A^1\Pi) + O$$

$$CS_2 + h\nu \rightarrow CS\ (A^1\Pi) + S$$

Although the production cross sections for some of these fragments are small, fluorescence from the excited fragments is observable and the vibrational populations should be measureable. As an example of the application of such data it should be noted that the mechanism for the production of the vibrational population of CO ($A^1\Pi$) as measured by the Mariner 6 and 7 UV spectrometer* has not yet been clarified. Photodissociation of CO_2 by solar radiation at $\lambda<1000$Å is thought to be the dominant mechanism. Measurement of the vibrational population produced by photodissociation is indeed required to help clarify the observed processes.

*C. A. Barth, C. W. Hord, J. B. Pearce, K. K. Kelly, C. P. Anderson and A. I. Stewart, J. Geophys. Res. 76, 2213 (1971).

IV. MEASUREMENT OF ELECTRONIC TRANSITION MOMENTS

The electronic transition dipole moments for the CO^+ ($A^2\Pi_i$, $B^2\Sigma^+ \rightarrow X^2\Sigma^+$), N_2^+ ($B^2\Sigma_u^+ \rightarrow X^2\Sigma_g^+$), and CO_2^+ ($A^2\Pi_u \rightarrow X^2\Pi_g$) systems have been measured in the previous funding period (see appendix A, H, I). For the diatomic systems the transition dipole moment was found constant but for the CO_2^+ system it fluctuated drastically. The transition dipole moment is a principal factor in the determination of band strengths and its measurement is important to the investigation of emission bands in planetary atmospheres. Transition dipole moments for the CO ($A^1\Pi \rightarrow X^1\Sigma$), N_2 ($B^3\Pi_g \rightarrow A^3\Sigma_u^+$), N_2 ($C^3\Pi_u \rightarrow B^3\Pi_g$), and CS ($A^1\Pi \rightarrow X^1\Sigma$) systems will be measured during the next funding period.

Franck-Condon factors for transitions in linear triatomic molecules are quite limited. Measurements of the band strengths for these transitions will hopefully stimulate reliable calculations of the Franck-Condon factors of interest.

V. STUDY OF THE PRESSURE DEPENDENCE OF THE FLUORESCENCE INTENSITY

The pressure dependence of the CO_2^+ ($B^2\Sigma_u^+ \rightarrow X^2\Pi_g$) and CO_2^+ ($A^2\Pi_u \rightarrow X^2\Pi_g$) fluorescence was measured during the previous funding period, and the two systems were found to yield similar results. No collisional "dumping" from CO_2^+ ($B^2\Sigma_u^+$) to the CO_2^+ ($A^2\Pi$) states was observed.

To simplify the analysis of the pressure dependence data, a uniform gas pressure inside the gas cell is required. Accordingly, an aluminum thin film was used to separate the gas cell from the main chamber of our normal incidence monochromator McPherson 225. However, the resulting reduction of the light incident on the gas cell to only 5% of the windowless intensity resulted in an unacceptably low fluorescence intensity for the individual bands. A revision of the present detection system to a more sensitive photon counting system is planned, and will be pursued during the next funding period. Measurement of the pressure dependence of the fluorescence intensity for planetary gases may aid in a determination of the pressure of such gases in planetary atmospheres.

VI. IDENTIFICATION OF UNCLASSIFIED MOLECULAR BANDS

Identification of vibrational bands of the N_2O^+ [$A^2\Sigma^+(0,0,0) \rightarrow X^2\Pi(n_1,n_2,n_3)$] system has been a part of our work during the previous funding period (see appendix J). The conventional methods (gaseous discharges) for exciting the gas whose spectrum is to be analyzed invariably yield numerous emission bands and atomic lines from the molecules and their fragments. In the present work a monochromatic photon beam is used to produce photoionization excitation and accordingly a relatively simple spectrum results, permitting unambiguous analysis. A determination of the vibrational bandhead positions is not proposed as a primary effort; it is a natural extension of our other work.

REFERENCES

Bates, D. R. and A. Dalgarno, J. Atm. Terr. Phys. 5, 329 (1954).

Cook, G. R. and P. H. Metzger, J. Opt. Soc. Amer. 54, 968 (1964).

Filseth, S. V. and K. H. Welge, J. Chem Phys. 51, 839 (1969).

Matsunaga, F. M. and K. Watanebe, Sci. Light 16, 37 (1967).

Melton, L. A. and W. Klemperer, Planet. Space Sci. 20, 157 (1972).

Schaeffer, R. C., P. D. Feldman, and E. C. Zipf, J. Geophys. Res. 77, 6828 (1972).

Slanger, J. G. and G. Black, J. Chem. Phys. 54, 1889 (1971)

Tanaka, Y., J. Chem. Phys. 20, 1728 (1952).